VŠB – TECHNICAL UNIVERSITY OF OSTRAVA

UNIVERSITY STUDY PROGRAMMES

Description and optimization of front glass in car headlights

Popis a optimalizace zobrazení čelních skel světlometů

Author: Bc. Jiří Dědek

Head of diploma thesis: doc. Dr. Mgr. Kamil Postava

Consultant: Mgr. Petr Ferbas

Ostrava 2018

VŠB - Technical University of Ostrava
University Study Programmes
CNT - Nanotechnology Centre

Diploma Thesis Assignment

Student: **Bc. Jiří Dědek**

Study Programme: N3942 Nanotechnology

Study Branch: 3942T001 Nanotechnology

Title: Description and optimization of front glass in car headlights
Popis a optimalizace zobrazení čelních skel světlometů

The thesis language: English

Description:

Proper functionality of front cover and imaging glasses is essential for a correct imaging of car headlights. The main target of the Master thesis is to describe, analyze, and design of the cover glasses. The thesis will be prepared in the frame of collaboration with the Varroc Lighting Systems company. The main aims:

1. Summarize description of energetic quantities and their relation to ray tracing in optical system (reflector and projection system). Description includes illumination of modern light sources as light emitting diodes (LEDs).
2. Description of the cover glass imagination on the basis of ray (geometrical) optics including its thickness, refractive index, and surface curvatures. The aim is to express the effects of projection on the space illumination and to show an example of ray tracing and its deviation influenced by two curved (spherical) surfaces.
3. General description will be applied to special kinds of cover glasses and to deformation of space illuminated by meeting headlight by using special shape of the cover glass. The Expose software from Varroc Co. will be applied to design of the cover glass shape.
4. Results will be verified using simulation software LightTools with the real meeting beam according to ECE112. The thesis will provide summary recommendation for design of the headlight cover glasses with relation to production.

References:

B. E. A. Saleh, M. C. Teich, Fundamentals of Photonics, 2nd ed., Willey, 2007.

D. J. Brady, Optical Imaging and Spectroscopy, 1st Ed., Willey, 2009.

R. Lenk, C. Lenk, Practical lighting design with LEDs, 2nd ed., John Wiley & Sons, 2017.

B. Wördenweber, J. Wallaschek, P. Boyce, D. Hoffman, Automotive Lighting and Human Vision, Springer-Verlag Berlin Heidelberg 2007.

Extent and terms of a thesis are specified in directions for its elaboration that are opened to the public on the web sites of the faculty.

Supervisor: **doc. Dr. Mgr. Kamil Postava**

Consultant: Mgr. Petr Ferbas

Date of issue: 26.10.2017

Date of submission: 21.05.2018

prof. Ing. Jaromír Pištora, CSc.
Head of Department

Ing. Zdeňka Chmelíková, Ph.D.
Vice-rectress for Study Affairs

Declaration

I declare I have elaborated this thesis by myself. All literary references and publication I have used had been cited.

In Ostrava: 18. 5. 2018 .....Jiří Dědek.....

Prohlášení

Byl jsem seznámen s tím, že na moji diplomovou práci se plně vztahuje zákon č.121/2000 Sb. – autorský zákon, zejména §35 – užití díla v rámci občanských a náboženských obřadů, v rámci školních představení a užití díla školního a §60 – školní dílo.

Beru na vědomí, že Vysoká škola báňská – Technická univerzita Ostrava (dále jen VŠB – TUO) má právo nevýdělečně ke své vnitřní potřebě diplomovou práci užít ($35 odst. 3).

Souhlasím s tím, že jeden výtisk diplomové práce bude uložen v Ústřední knihovně VŠB – TUO k prezenčnímu nahlédnutí a jeden výtisk bude uložen u vedoucího diplomové práce. Souhlasím s tím, že údaje o diplomové práci budou zveřejněny v informačním systému VŠB – TUO.

Bylo sjednáno, že s VŠB – TUO, v případě zájmu z její strany, uzavřu licenční smlouvu s oprávněním užít dílo v rozsahu §12 odst. 4 autorského zákona.

Bylo sjednáno, že užít své dílo – diplomovou práci nebo poskytnout licenci k jejímu využití mohu jen se souhlasem VŠB – TUO, která je oprávněna v takovém případě ode mne požadovat přiměřený příspěvek na úhradu nákladů, které byly VŠB – TUO na vytvoření díla (až do jejich skutečné výše).

Beru na vědomí, že odevzdáním své práce souhlasím se zveřejněním své práce podle zákona č. 111/1998 Sb., o vysokých školách a o změně a doplnění dalších zákonů (zákon o vysokých školách), ve znění pozdějších předpisů, bez ohledu na výsledek obhajoby.

In Ostrava: 18.5.2018 ..... Jiří Dědek

Student's signature

Name and surname of author: Jiří Dědek

Permanent address of author: Mniší 114, Kopřivnice, 74221

Acknowledgment

I would like to express my big gratitude to my supervisor doc. Dr. Mgr. Kamil Postava for his patience and his useful advices that he gave to me, my consultant Mgr. Petr Ferbas for his surveillance over technical and practical part in Varroc Lighting Systems, s.r.o. and my colleagues in Varroc Lighting Systems, s.r.o., especially Ing. Petr Němec who gave me a lot of advices and ideas to my thesis. I would also like to thank my girlfriend Jana for her endless support and patience, this thesis is dedicated to her. Last but not least I would like to thank my family for a great support, without them, this thesis would not be created.

Anotace

Tato diplomová práce je zaměřena na popis a optimalizaci krycích skel světlometů. V první části se nachází obecný popis světlometu, užívané optické systémy, světelné zdroje v automobilovém průmyslu a materiál krycího skla, dále je zde zmíněna oblast fotometrie a její veličiny a poté computer-aided design a používaný software v této práci. Druhá část zahrnuje popis optiky krycího skla, konkrétně analytický výpočet odchylky světelného paprsku po průchodu krycím sklem, vypočtení odrazivosti a popis intenzitního rozložení. Hlavní část této práce řeší metodu optimalizace krycích skel užitím software ve spolupráci s firmou Varroc Lighting Systems, s.r.o. a vytvořením směrnice pro postup této optimalizace.

Klíčová slova:

krycí sklo, světlomet, optimalizace, CATIA, analýza, odchylka paprsku

Vzor citace:

DĚDEK, Jiří. *Description and optimization of front glass in car lighting*. Ostrava, 2018. Diplomová práce. Vysoká škola báňská – Technická univerzita Ostrava. Vedoucí práce doc. Dr. Mgr. Kamil Postava

Annotation

This diploma thesis is focused on description and optimization of front glass in car lighting. In the first part there is general description of headlamp, used optical systems, light sources in automotive industry and material of cover glass, next there is mentioned photometry and its units and further computer-aided design and used software in this thesis. The second part consists of description of optics of cover glass, specifically analytical calculation of deviation of light beam on passage of cover glass, calculation of reflectance and description of intensity layout. The main part of this thesis is method of optimization of cover glass using software in a cooperation with company Varroc Lighting Systems, s.r.o. and creating a guideline for process of this optimization.

Key words:

cover glass, headlamp, optimization, CATIA, analysis, beam deviation

Reference format:

DĚDEK, Jiří. *Description and optimization of front glass in car lighting*. Ostrava, 2018. Diploma thesis. VŠB – Technical University of Ostrava. Supervisor doc. Dr. Mgr. Kamil Postava.

Contents

1. Introduction

Optimization of cover glass is an important suspect in a procedure of proposal a new headlamp. This diploma thesis is made in a cooperation with the company Varroc Lighting Systems, s.r.o. This company had a need for creating a comprehensive guideline for a procedure of optimization of cover glass, therefore that is a main objective of this thesis. Despite of cover glass of headlamp significantly affects its luminous properties and functionality in general, there is a lack of information about cover glass optics and optimization in books and technical journal.

The motivation for optimization of cover glass is to create an optical interface that will minimalize the beam deviation, will have fine viewing properties and better results regarding photometry and gradient aiming. To be able to obtain this optimized cover glass we need to understand and describe the optics of cover glass, optical systems in headlamps and their light sources and used material for cover glass. For a purpose of optimization, we need to learn computer-aided design and master specific commercial and company internal software. We also need to use specific software for analysis of cover glass to be able to discuss results and used methods.

This thesis is organized as follows. In Chapter 2 we describe general function of headlamp, used optical systems, light sources in automotive industry and material of cover glass used in Varroc Lighting Systems, s.r.o. Photometry and its importance with its units, and further computer-aided design and used software in this thesis are reviewed in Chapters 3 and 4, respectively. Chapter 5 deals with description of optics of cover glass, specifically analytical calculation of deviation of light beam on passage of cover glass, all relations are clearly listed, calculation of reflectance and description of intensity layout. The main part of this thesis is in Chapter 6 and it is method of optimization of cover glass using software in a cooperation with company Varroc Lighting Systems, s.r.o. and creating a guideline for process of this optimization. After this part there is discussion of results and last chapter consists conclusion and perspectives for future.

2. Headlamp description

This chapter contains description of headlamps, their optical system, light sources which are used nowadays, and type of material used for cover glass.

A headlamp is the term for device that is attached to the front of a vehicle and is lighting the road ahead. The term headlight refers to the beam of light which is produced and distributed by the device. Modern headlamps are electrically operated and positioned in pairs with one or two on each side of the vehicle. The whole system of headlamp is required to produce a high and low beam, which is achieved by a multi-function lamp or by an individual lamp for each function. High beams maximize seeing distance and therefore cast most of their light straight ahead, however they produce too much glare for safe use when there are other vehicles on the road. Low beams have stricter control of upward light than high beams and that is why they direct most of their light downward and either rightward or leftward, depending on specific country. They provide safe forward visibility without backdazzle or excessive glare [1].

The headlamp generally consists of optical system, light source and cover glass, all parts will be described subsequently.

2.1. Optical system

There are two main optical systems used in automotive industry, specifically reflector and projector modules, both systems are equally important and both are described subsequently.

2.1.1. Reflector lamps

In this optical system we have two types of optics, lens and reflector optics, which are schematically shown in Figure 1. The lens optics is practically not used nowadays, in this optical system a light source is placed near focus point of a reflector, which has a parabolic or non-parabolic complex shape. Prism and Fresnel optics moulded into the headlamp lens refract parts of the light laterally and vertically to obtain the required light distribution pattern [2]. Reflector optics, the most common optical system now, started to develop in the 1980s. CAD technology, which will be described later, allowed the development of reflector headlamps with nonparabolic, complex-shape reflectors. The optics to distribute the light in the required pattern are designed into the reflector itself. The entire surface area is modified to produce individual segments of complex, specifically calculated contours. The cumulative effect from the shape of each designed

segment produces the desired light distribution pattern. Modern reflectors are often made of injection moulded or compression-moulded plastic, the specific material used in Varroc Lighting Systems s.r.o. will be discussed later. The reflective surface is from vapor deposited aluminum, with a clear overcoating preventing the extremely thin aluminum from oxidizing [3].

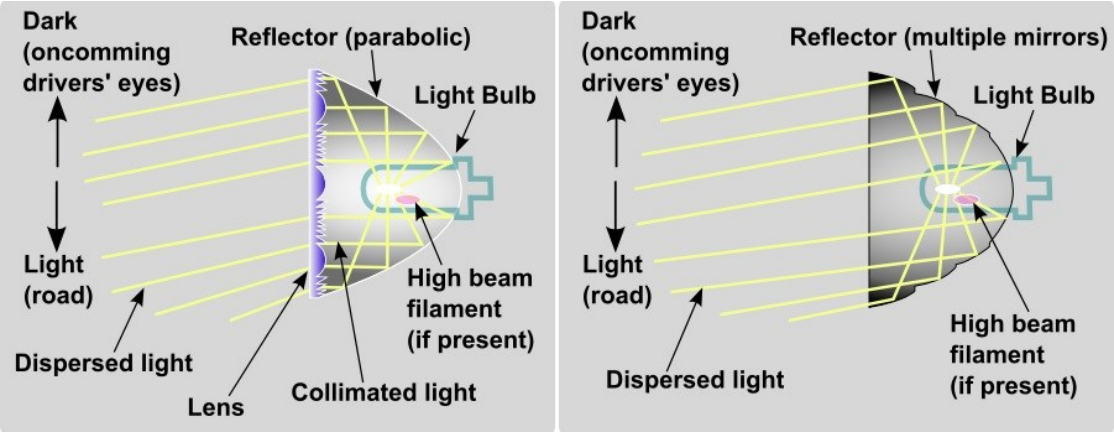

Figure 1: Two types of reflector systems,
on the left is lens optics and on the right is reflector optics [4]

2.1.2. Projector (polyellipsoidal lamps)

This system has a light source located at one focus point of an ellipsoidal reflector and a condenser lens at the front of the lamp, as it is shown in Figure 2. Between reflector and lens is located a shield at the image plane and the projection of the top edge of this shield provides the low-beam cutoff. The shield can be removed from the light path for high beam and lowered by a solenoid actuated pivot to provide low beam. These optics systems are known as bifunctional projectors.

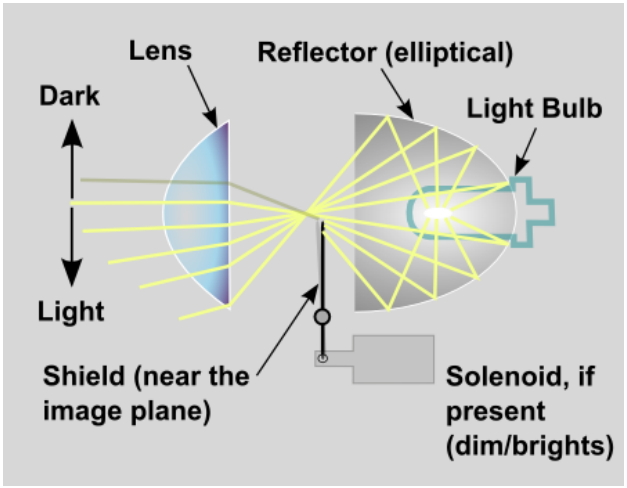

Figure 2: Projector optics system of headlamp [4]

To reduce sharpness the condenser lens may have slight Fresnel rings or other surface treatments. Projector main headlamps first appeared in 1980s, the projector low beam permitted accurate beam focus and a much smaller-diameter optical package, though a much deeper one, for any given beam output. The main disadvantage of this type of headlamp is the urge to accommodate the physical depth of the assembly, which may extend far back into the engine compartment, therefore it demands a lot of space [5].

2.2.Light sources

In this section we summarize light sources used in automotive industry, basically there are two most important sources nowadays, traditional bulb sources and the most common used sources at this time, light-emitting diode (LED) sources.

2.2.1. Incandescent light bulb

An incandescent light bulb or incandescent lamp is an electric light with a wire filament heated to such a high temperature that it glows with visible light (incandescence). The filament is protected with a glass or fused quartz bulb that is filled with inert gas or evacuated to prevent from oxidation. For a halogen lamp is filament evaporation slowed by a chemical process that redeposits metal vapor onto the filament which extends its life. Incandescent bulbs are produced in a variety of range of sizes, light output and voltage ratings from 1,5 volts to even 300 volts. They have low manufacturing costs and work equally well on either alternating or direct current, but they are much less efficient than other types of electric lighting, because they convert less than 5% of the energy they use into the visible light. The luminous efficacy, which will be discussed in photometry, of a typical incandescent bulb is 16 lumens per watt [6].

Bulb sources in automotive industry

There are several standardized series of light bulbs that are made for automobiles. Bulbs that are used for headlamps, brake lamps and turn signals are required to comply with national and international regulations governing the types of used lamps. Auxiliary lamps, interior lighting or other automotive lighting applications are not regulated, but there are some common types of bulbs that are used by many automotive producers. The international-consensus UN Regulations on light sources is developed and maintained by the World Forum for Harmonization of Vehicle Regulations (ECE Regulations) and is acceptable for use in lamps on vehicles and trailers for use in countries that recognize the UN Regulations. UN Regulation 37 contains motor vehicle filament lamps divided

in three groups: without general restriction, acceptable only for signaling lights and no longer allowable as light sources for new type approvals but still permitted as replacement parts. From these groups we can name examples like bulbs H2, H4, H7, S2, H6W, P21W [7]. Figure 3 shows example of H7 light bulb for headlamp.

Figure 3: H7 light bulb from Philips [8]

UN Regulation 99 contains gas discharge light sources for use in vehicle headlamps, all light sources acceptable there are also acceptable under US regulations. From this regulation we can name examples like D1R, D2R, D2S or D4S.

2.2.2. Light-emitting diode

Nowadays the light-emitting diode (LED) sources are the most used sources of light in the automotive industry, and therefore we will focus our attention on them. LED is a two-lead semiconductor, specifically it is a p-n junction diode that emits light when activated. One of many benefits of LEDs is their size (less than 1 mm^2) and that is why integrated optical components may be used to shape the radiation pattern. Modern LEDs work with very high brightness and are available across the infrared, visible and ultraviolet wavelengths, in addition LEDs have led to new displays and sensors, while their high switching rates are useful in advanced communications technology. Comparing the advantages of LEDs over incandescent light sources, we can mention longer lifetime, lower energy consumption, faster switching, improved physical robustness and smaller size. Currently the LED lights home room lighting are as cheap

or cheaper than compact fluorescent lamp sources of comparable output, also they have fewer environmental concerns linked to their disposal and are much more energy efficient. The colour of light emitted from the LED is neither monochromatic nor coherent like it is in laser, but the spectrum is narrow with respect to human vision and the light from a simple diode element can be for most purposes regarded as functionally monochromatic [9].

Working principle

LEDs are working on phenomenon generally called electroluminescence, which basically means, that the p-n junction emits light when electrical energy is applied to it. The charge carriers recombine in a forward-biased p-n junction as the electrons cross from the n-region and recombine with the holes existing in the p-region. Holes are in the valence energy band, while free electrons are in the conduction band of energy levels.

The energy level of the holes is less than the energy levels of the electrons and therefore some portion of the energy must be dissipated to recombine the electrons and the holes. This energy is emitted in the form of light and heat. If the semiconductor is translucent, the junction becomes the source of light and thus becoming a light-emitting diode. The colour of the light (corresponds to the energy of the photon) is affected by the energy band gap of the semiconductor [10]. The working principle of LED is shown in Figure 4.

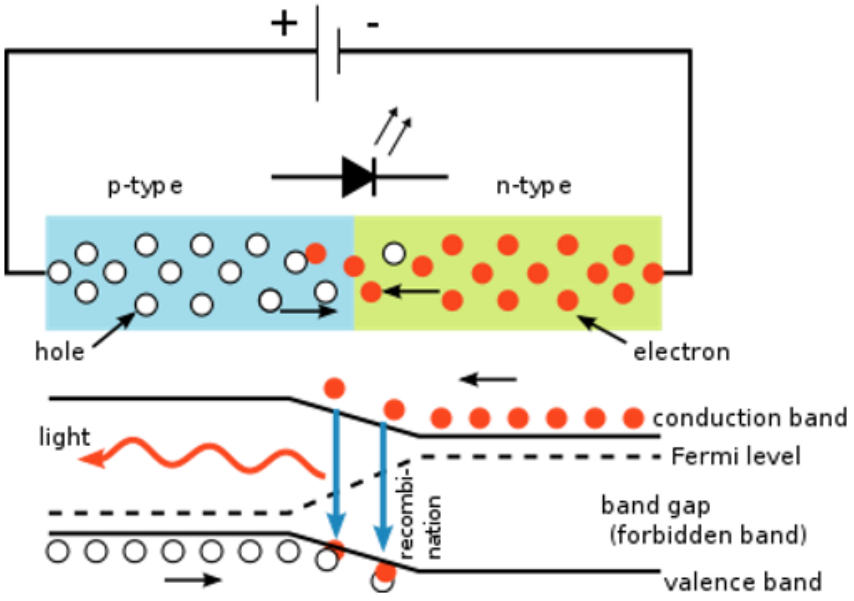

Figure 4: The inner workings of LED,
showing circuit (top) and band diagram (bottom) [11]

2.3. Material of cover glass

Cover glass of automotive forward lighting in Varroc Lighting Systems, s.r.o. is made from Bisphenol A – Polycarbonate (PC), its chemical formula is shown in Figure 5.

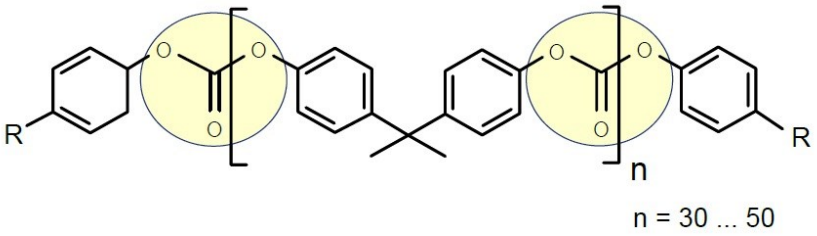

Figure 5: Chemical formula of Bisphenol A – Polycarbonate

It is clear and transparent like glass, its properties are exceptionally high dimensional accuracy and stability, high notched impact strength, isotropic behavior, heat resistance to temperature up to 148°C, resistance to ignition sources and many more. There are specifically two PC materials which are used in our company, the first is Makrolon® AL2647 and the second is LEXAN™ Resin LS1. AL2647 has refractive index in value of 1,587, LS1 in value of 1,586, we can see that they are almost the same, but later in our calculations we will use the value of 1,586. One of important parameters is luminous transmittance, dependence for AL2647 is shown in Figure 6. The sirface of cover glass is protected by a thin film on the surface of glass called hard coat which improves abrasion and scratch resistance and weatherability and UV protection. Requirements for hard coat are adhesion, transparency and chemical resistance. Coating techniques used for this thin film are gas phase deposition (PVD and PECVD) and liquid phase deposition (dip coating, spray coating, spin coating,…) [12].

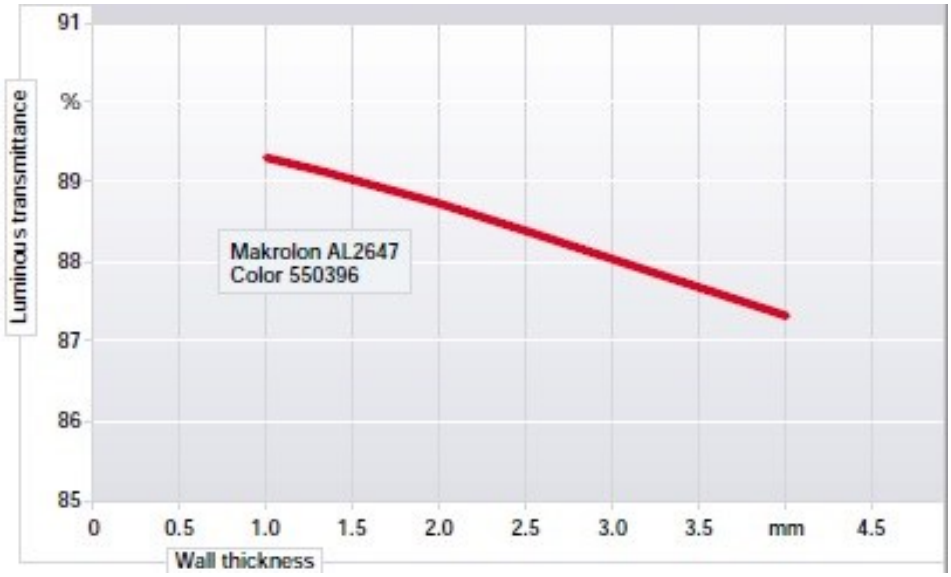

Figure 6: Dependence of luminous transmittance on wall thickness of glass [13]

3. Photometry in lighting industry

In this chapter we will explain what a photometry is and what is its importance in lighting industry.

Photometry describes measurement of electromagnetic radiation weighted by the response of human eye. This response changes from person to person, or with wavelength. Internationally-agreed standard observer functions are therefore used in order to provide a consistent measurement base for photometry. In photometry, the word 'luminous' is used to indicate that measurements have been made using a detection system (called a photometer) that has a spectral response similar to that of a human eye [14].

3.1. Photometry units

In photometry we use five basic quantities, namely luminous flux, luminous intensity, illuminance, luminance and luminous efficacy.

Luminous flux

It describes total energy of light source (electromagnetic source) perceived by human eye, reflecting varying sensitivity to different wavelengths. It differs from radiant flux, the measure of the total power of electromagnetic radiation. The International System of Units (SI) of luminous flux is the lumen (lm). One lumen is defined as the luminous flux of light produced by a light source that emits one candela of luminous intensity over a solid angle of one steradian. In other systems of units, luminous flux may have units of power. The luminous flux accounts for the sensitivity of the eye by weighting the power at each wavelength with the luminosity function, which represents the response of eye to different wavelengths. Luminous flux is a weighted sum of the power at all wavelengths in the visible band, light outside the visible band does not contribute. Luminous flux is often used as an objective measure of the useful light emitted by a light source and is typically reported on the packaging for light bulbs. Luminous flux is not used to compare brightness, as this is a subjective perception which varies according to the distance from the light source and the angular spread of the light from the source. The relation between luminous flux and luminous intensity is that the luminous flux is a measure of the total amount of light a lamp puts out and the luminous intensity is a measure of how bright the beam in a particular direction is.

The luminous flux Φ is defined as:

$$\phi = K(\lambda) \cdot \phi_e(\lambda) \,, \tag{3.1}$$

where $K(\lambda)$ is the luminous efficacy of monochromatic light and $\phi_e(\lambda)$ is the radiant flux [15]. The luminous efficacy $K(\lambda)$ of an eye is shown in Figure 7.

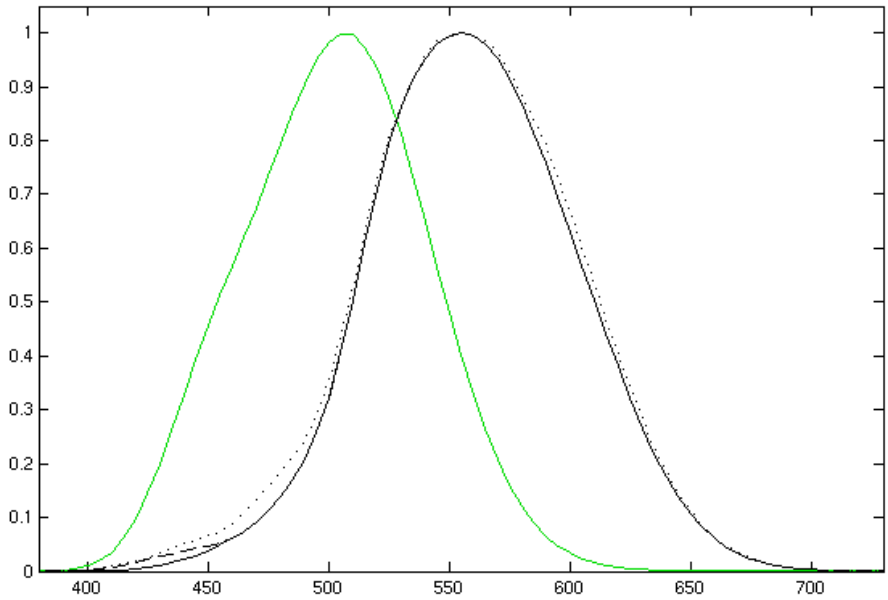

Figure 7: Dependence of normalized luminous efficacy on wavelength

The green line represents scotopic (low lighting levels) luminosity function [16] and the black line represents photopic (day-time light levels) luminosity function [17].

Luminous intensity

It describes a measure of the wavelength-weighted power emitted by a light source in a particular direction per unit solid angle, which is expressed in steradians (sr). Schematic view of 1 sr is shown in Figure 8. The SI unit of luminous intensity is the candela (cd).

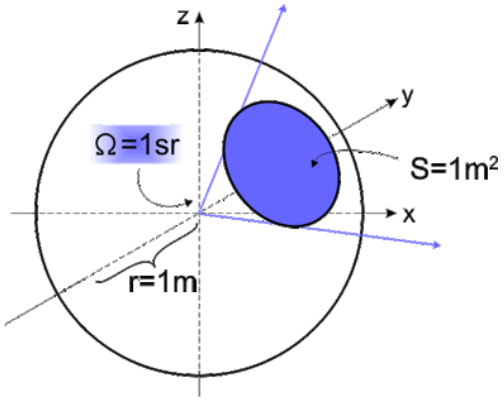

Figure 8: The preview of luminous intensity on solid angle of 1sr

Luminous intensity *I* is defined as follows:

$$I = \frac{d\phi}{d\Omega}, \tag{3.2}$$

where $d\Omega$ is the solid angle [18].

Illuminance

Illuminance describes the total luminous flux perpendicularly incident on a surface, per unit area. It is a measure of how much the incident light illuminates the surface, wavelength-weighted by the luminosity function to correlate with human brightness perception. In SI derived units the unit of illuminance is lux or lumen per square meter and the relation of illuminance *E* is:

$$E = 10^{\frac{(-14{,}18-M_v)}{2{,}5}}, \tag{3.3}$$

where *Mv* is the apparent magnitude [19].

Luminance

Luminance is defined as a photometric measure of the luminous intensity per unit area of light travelling in a given direction. It describes the amount of light that passes through, is emitted or reflected from a particular area, and falls within a given solid angle. It is used to describe primary and secondary planar light sources. The SI unit for luminance is candela per square meter. The luminance *L* of a reflecting surface is related to the illuminance by relation:

$$\int_{\Omega_\Sigma} L \mathrm{d}\Omega_\Sigma \cos\theta_\Sigma = ER, \tag{3.4}$$

where the integral covers all the directions of emission Ω_Σ, which is solid angle containing the specified direction, θ_Σ is is the angle between the normal nΣ to the surface dΣ and the specified direction, *E* is illuminance and *R* is reflectance [20].

Luminous efficacy

Luminous efficacy is a measure of how well a light source produces visible light. It is the ratio of luminous flux to power, measured in lumens per watt in the SI units. Depending on context, the power can be either the radiant flux of the source's output, or it can be the total power (chemical energy, electric power or others) consumed by the source. Luminous efficacy, denoted *K* is defined as:

$$K = \frac{\phi_v}{\phi_e}, \tag{3.5}$$

where ϕ_v is the luminous flux and ϕ_e is the radiant flux [21].

Table 1: Photometric quantities

Name	Symbol	Unit	Explanation
Luminous flux	ϕ	lm	Total light power incident on a surface, energy of light per unit time, considering human eye varying sensitivity
Luminous intensity	I	cd	Luminous flux emitted in a given solid angle
Illuminance / Illumination	E	lx	Total luminous flux incident upright on an illuminated surface
Luminance / Brightness	L	$cd \cdot m^{-2}$	Luminous intensity emitted from a surface
Luminous efficacy	K	$lm \cdot W^{-1}$	Ratio of usable light to total electrical input of a light source

3.1.1. Illuminance of real light source

We will apply photometric units to rays of light and describe layout of light intensity in space. At first we will focus on a general comparison of the luminous flux, intensity and illuminance, which is shown in Figure 9.

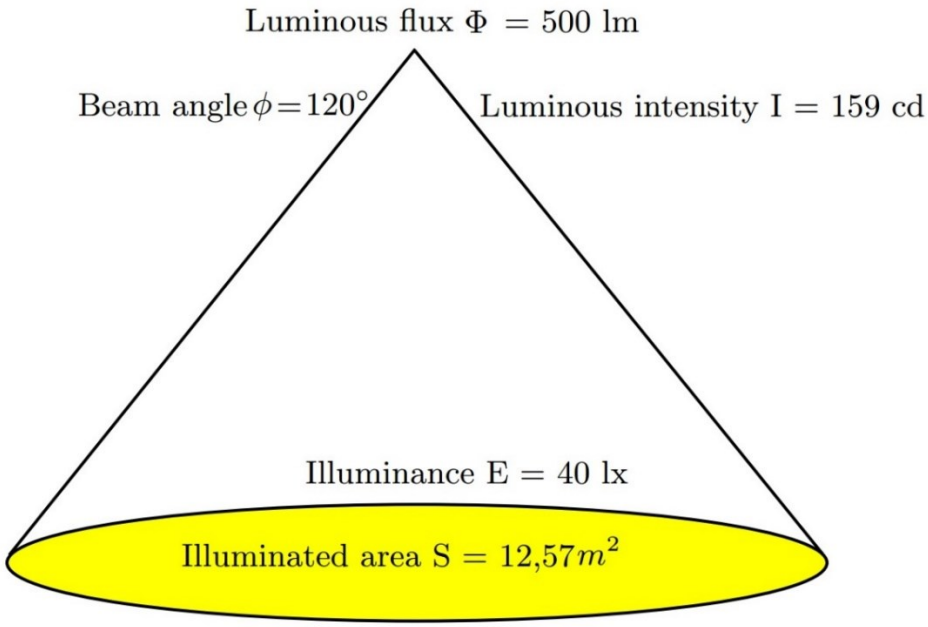

Figure 9: Comparison of luminous flux, intensity and illuminance

That is a general comparison, but when we would like to describe it more precisely we need to use the basic photometric law, which is shown in Figure 10.

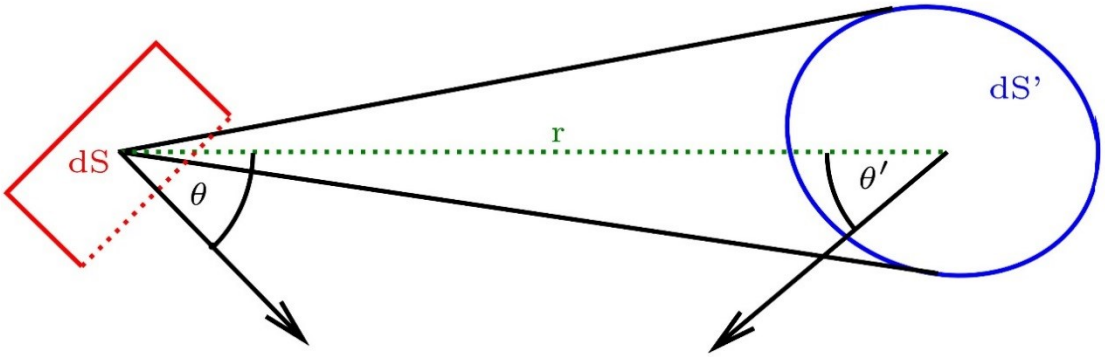

Figure 10: Basic photometric law

Its formula is:

$$d\phi_e = E_e dS dS' \frac{\cos\theta \cos\theta'}{r^2}, \tag{3.6}$$

where ϕ_e is luminous flux and E_e is illuminance. This dependence of illuminance will be very important for our future analysis. In a real light source used in headlamps the number of light rays is in millions and it is quite difficult to illustrate the illuminance of real light source. Fortunately, the software Beam Analyzer, developed in Varroc Lighting Systems, s.r.o. can visualize the illuminance of light source on 25 meter sphere. This is shown in Figure 11 and we can clearly see the layout of illuminance. Later we will use this software to compare illuminances between headlamps with different setups.

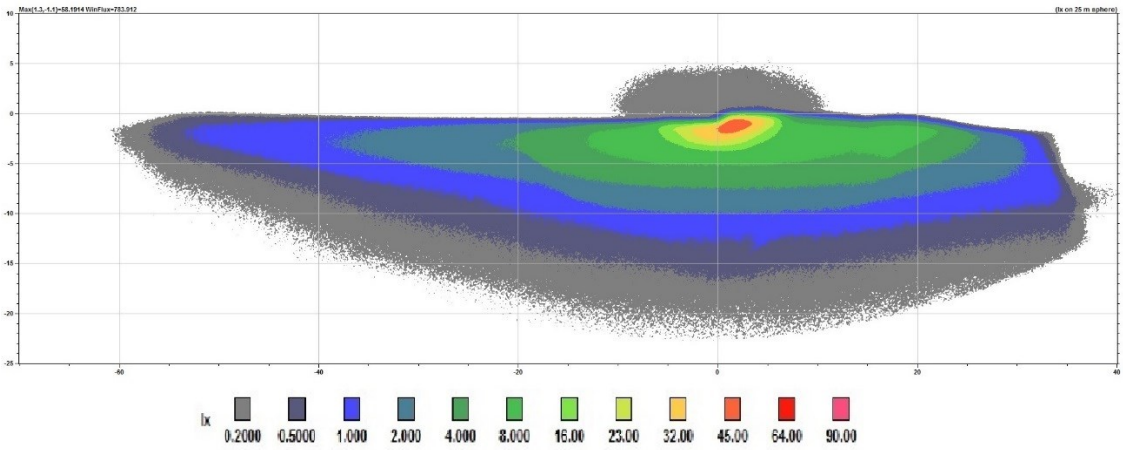

Figure 11: Illuminance of real beam pattern in headlamp

4. Computer-aided design and used software

In this chapter is summary of software used in this diploma thesis, basics how they operate and the definition of computer-aided design, which is the foundation stone for all computer modelling.

4.1. Computer-aided design (CAD)

Computer-aided design (CAD) is a use of workstations or computer systems to help in the creation, modification, analysis or optimization of a design. CAD software is used to improve the quality of design, increase the productivity of the designer and to create a database for manufacturing. Output of the CAD is often in the form of electronic files for manufacturing operations like print or machining. For mechanical design the CAD software uses vector-based graphics to depict the objects of traditional drafting or may also produce raster graphics showing the overall appearance of designed objects. In manual drafting of engineering and technical drawings the CAD output must convey information such as processes, materials, dimensions and tolerances according to application-specific conventions. We may use CAD to design figures and curves in two-dimensional space or surfaces, curves and solids in three-dimensional space, second option is more frequent for application in car lighting [22]. CAD has become very important technology within the scope of computer-aided technologies, with benefits such as greatly shortened design cycle and lower product development costs. It enables designers to develop and layout work on screen, print it and save for future editing, which is valuably saving time on their drawings. Technology of CAD systems has radically change since the beginning of its development, modern CAD system can be seen as built up from the interaction of a graphical user interface with NURBS geometry or boundary representation data via a geometric modeling kernel [23]. In Varroc Lighting Systems s.r.o. the CAD system CATIA from company Dassault Systèmes is used.

4.1.1. CATIA

CATIA (computer-aided three-dimensional interactive application) is a multi-platform software suite for CAD, computer-aided engineering (CAE), computer-aided manufacturing (CAM) developed by the French company Dassault Systèmes. It started as an in-house development in 1977 by French aircraft manufacturer Avions Marcel Dassault.

Concerning mechanical engineering, CATIA enables the creation of 3D parts, 2D sketches, composites, sheetmetal, molded, forged or tooling parts and the definition of mechanical assemblies, concerning the design, it offers a solution to shape design, styling, surfacing workflow and visualization to create, modify and validate complex innovative shapes. CATIA can be used in a wide variety of industries, for example defense, aerospace, automotive, industrial equipment, high tech, consumer goods, shipbuilding, plant design, life sciences, construction, architecture, process power, petroleum and services [24].

CATIA has the unique ability to model any product and also to do it in the context of its real-life behavior, that means design in the age of experience. Designers, engineers, systems architects and all contributors can imagine, shape and define the connected world. Amongst others CATIA delivers an instinctive 3DEXPERIENCE, for both occasional and experienced users with world-class 3D simulation and modelling capabilities that optimize the effectiveness of every user, a social design environment built on a single source of truth and accessed through powerful 3D dashboards that drive real-time concurrent design, business intelligence and collaboration across all stakeholders including mobile workers, and an inclusive product development platform that is easily integrated with existing tools and processes. This enables multiple disciplines to leverage integrated and powerful specialist applications across all phases of the product development process. CATIA's Engineering, Systems Engineering and Design applications are the heart of Industry Solution Experiences from Dassault Systémes to address all industry needs. It revolutionizes the way organizations create, develop and realize new products and therefore delivering competitive edge through innovative customer experience [25].

4.2. EXPOSE

EXPOSE is a system of software that was developed in Varroc Lighting Systems, s.r.o. and it allows to create and analyze optical surfaces. The system is based on dynamically loaded libraries called modules that allow to incorporate algorithms without the need to reinstall the system. It has a various number of applications. In this diploma thesis, the EXPOSE software is used for creating optimized neutral surface of lens.

4.3. LucidShape

LucidShape is the most powerful and advanced computer aided lighting design software for automotive lighting design tasks according to a producer, which is Synopsys. LucidShape facilitates the design of automotive forward, rear and signal lighting and reflectors with dedicated algorithms optimized especially for automotive applications [26]. We use LucidShape in this diploma thesis for analysis of ray deviation of cover glass.

4.4. LuxRender

LuxRender is a physically based and unbiased rendering engine, and based on state of the art algorithms, simulates the flow of light according to physical equations and thus producing realistic images of photographic quality. It models the transportation of light which allows it to accurately capture a wide range of phenomena [27]. In this diploma thesis we use LuxRender in association Blender software for creating a realistic visualization of cover glass and its viewing properties.

4.5. LightTools

LightTools is design and 3D optical engineering software product that supports simulation, virtual prototyping, optimization and photorealistic renderings of illumination applications. It helps to ensure the delivery of illumination designs according to specifications and schedule [28]. For our diploma thesis is the most important function of LightTools the creation of map of light intensity, which we will analyze in Beam Analyzer software.

4.6. Beam Analyzer

Beam Analyzer is a software that was developed in Varroc Lighting Systems, s.r.o. for visualizing and analyzing the maps of light intensity that were created in LightTools software. It has many functions and properties, for us is the most important visualizing the layout of light intensity and the coordinates of the point with highest light intensity.

5. Description of optics of cover glass

In this chapter we will describe and analyze optics of cover glass using Snell law of refraction, reflection coefficients and light intensity of rays. At first we approximate cover glass with plane interfaces and derive general formula for beam deviation. Next we discuss special cases of plane interfaces and compare our calculated results with measured results from CATIA software. In next section we transform our relations to 3 dimensions and in last section we discuss optics of real cover glass.

5.1. Approximation of cover glass with plane interfaces

To understand the light propagation in cover glass, we will calculate the light refraction in the structure air – glass – air. The first approximation is assuming that the glass contains two planar surfaces, as we can see in Figure 12.

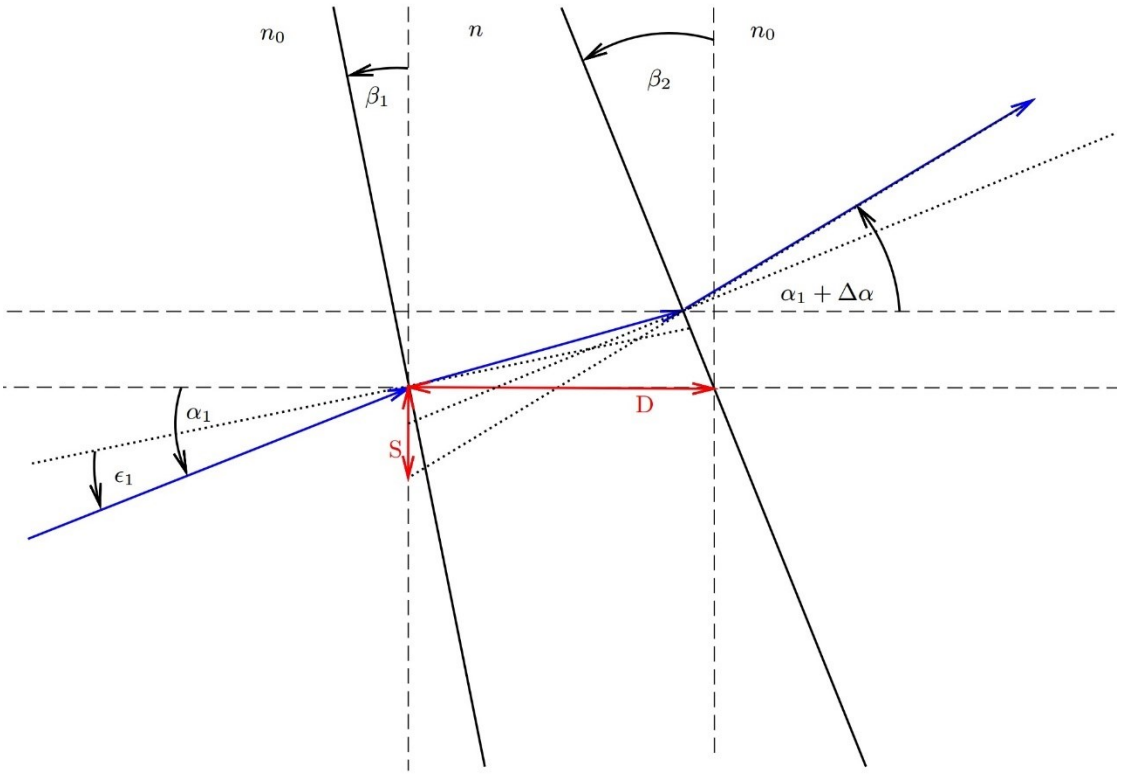

Figure 12: Scheme of light refraction on two planar surfaces

5.1.1. General formula of beam deviation

Our goal is to get formulas for calculation of two parameters, respectively the deviation angle $\Delta\alpha$ and the beam shaft parameter S, as shown in Figure 9. As was said earlier, that the structure is air – glass – air, the index of refraction n_0 for air is of value n_0=1.To obtain these parameters we must perform series of calculation. Let us start with the first refraction, detail is shown in Figure 13.

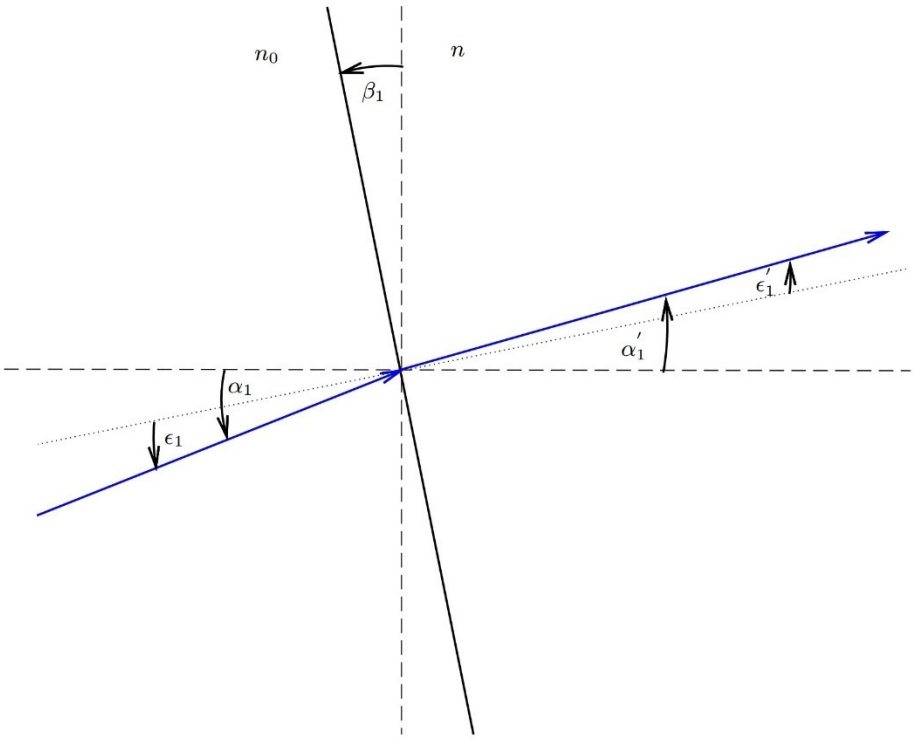

Figure 13: Scheme of first refraction

Using the Snell's law we obtain formulas for the first refraction:

$$\varepsilon_1' = \sin^{-1}\left(\frac{\sin\varepsilon_1}{\mathrm{n}}\right) \tag{5.1}$$

$$\alpha_1' = \beta_1 + \varepsilon_1' \tag{5.2}$$

$$\varepsilon_2 = \beta_1 + \varepsilon_1' - \beta_2, \tag{5.3}$$

and if we repeat the process, we get the similar formulas for the second refraction:

$$\varepsilon_2' = \sin^{-1}(\mathrm{n}\cdot\sin\varepsilon_2) \tag{5.4}$$

$$\alpha_2' = \beta_2 + \varepsilon_2'. \tag{5.5}$$

One of the goals is to get formula of the angle $\Delta\alpha$, which is:

$$\Delta\alpha = \alpha_2' - \alpha_1 = \beta_2 + \varepsilon_2' - \alpha_1 = \beta_2 - \alpha_1 + \sin^{-1}\left\{\mathrm{n}\cdot\sin\left[\beta_1 - \beta_2 + \sin^{-1}\left(\frac{\sin\varepsilon_1}{\mathrm{n}}\right)\right]\right\}. \tag{5.6}$$

And after implying the relation:

$$\varepsilon_1 = \alpha_1 - \beta_1, \tag{5.7}$$

we obtain the final relation of $\Delta\alpha$:

$$\Delta\alpha = \beta_2 - \alpha_1 + \sin^{-1}\left\{\mathrm{n}\cdot\sin\left[\beta_1 - \beta_2 + \sin^{-1}\left(\frac{\sin(\alpha_1-\beta_1)}{\mathrm{n}}\right)\right]\right\}. \tag{5.8}$$

The second goal is to derive the relation for the parameter *S*, which can be derived after some calculations using the laws in triangles and it can be written in the form:

$$S = \frac{\frac{D \cdot \cos\beta_2}{\cos(\beta_1 + \varepsilon_1' - \beta_2)} \cdot \sin(\beta_2 - \beta_1 + \varepsilon_2' - \varepsilon_1')}{\cos(\beta_2 + \varepsilon_2')} \tag{5.9}$$

And after using relations (5.1) – (5.5) and (5.7) we get the final formula of parameter S:

$$S = \frac{\frac{D \cdot \cos\beta_2 \cdot \sin\left\{\beta_2 - \beta_1 - \sin^{-1}\left[\frac{\sin(\alpha_1 - \beta_1)}{\mathrm{n}}\right] + \sin^{-1}\left[\mathrm{n} \cdot \sin\left(\beta_1 - \beta_2 + \sin^{-1}\left(\frac{\sin(\alpha_1 - \beta_1)}{\mathrm{n}}\right)\right)\right]\right\}}{\cos\left\{\beta_1 - \beta_2 + \sin^{-1}\left[\frac{\sin(\alpha_1 - \beta_1)}{\mathrm{n}}\right]\right\}}}{\cos\left\{\beta_2 + \sin^{-1}\left[\mathrm{n} \cdot \sin\left(\beta_1 - \beta_2 + \sin^{-1}\left(\frac{\sin(\alpha_1 - \beta_1)}{\mathrm{n}}\right)\right)\right]\right\}} \tag{5.10}$$

5.1.2. Special cases

Now let us discuss several special cases, which could happen, for example two parallel surfaces, normal incidence or the paraxial approximation of small angles.

Two parallel surfaces

The first special case is when we have two parallel surfaces, so $\beta_2 = \beta_1 = \beta$. The formulas change as follows:

$$\Delta\alpha = \beta - \alpha_1 + \sin^{-1}\left\{\mathrm{n} \cdot \sin\left[\sin^{-1}\left(\frac{\sin(\alpha_1 - \beta)}{\mathrm{n}}\right)\right]\right\} = 0, \tag{5.11}$$

$$S = \frac{\frac{D \cdot \cos\beta \cdot \sin\left\{\alpha_1 - \beta - \sin^{-1}\left[\frac{\sin(\alpha_1 - \beta)}{\mathrm{n}}\right]\right\}}{\cos\left\{\sin^{-1}\left[\frac{\sin(\alpha_1 - \beta)}{\mathrm{n}}\right]\right\}}}{\cos(\alpha_1)} \tag{5.12}$$

To prove that we have correct formulas, let us compare the values which we calculate from our formulas and the values we get from ray tracing function in CATIA. The inputs are β=15,945°, α_1=30°, D=40 mm and refractive index of glass n=1,586. When we put these values in our formulas, we get the outputs $\Delta\alpha$=0° and *S*=4,1098 mm. The values obtained from measurement in CATIA are in Figure 14, comparison of calculated and measured values is in Table 2.

Table 2: Comparison of calculated and measured values

Values	Calculated	Measured
Deviation angle $\Delta\alpha$ [°]	0	0
Beam shaft parameter *S* [mm]	4,1098	4,11

As we can see, the values match each other.

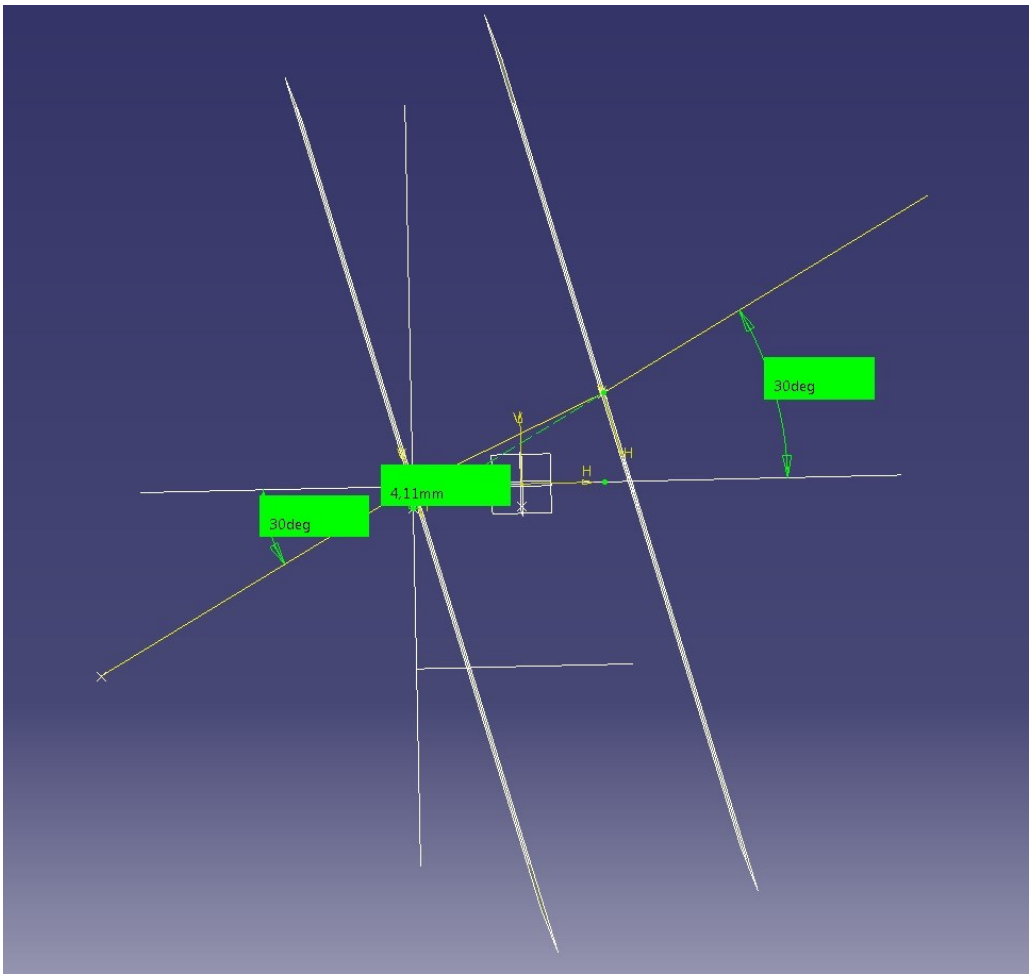

Figure 14: Values from CATIA in the first special case

Incidence with α_1=0°

The second special case which can happen is incident ray with angle α_1=0°. The formulas look differently again:

$$\Delta\alpha = \beta_2 + \sin^{-1}\left\{\mathrm{n}\cdot\sin\left[\beta_1 - \beta_2 + \sin^{-1}\left(\frac{\sin(-\beta_1)}{\mathrm{n}}\right)\right]\right\}, \tag{5.13}$$

$$S = \frac{D\cdot\cos\beta_2\cdot\sin\left\{\beta_2 - \beta_1 - \sin^{-1}\left[\frac{\sin(-\beta_1)}{\mathrm{n}}\right] + \sin^{-1}\left[\mathrm{n}\cdot\sin\left(\beta_1 - \beta_2 + \sin^{-1}\left(\frac{\sin(-\beta_1)}{\mathrm{n}}\right)\right)\right]\right\}}{\cos\left\{\beta_1 - \beta_2 + \sin^{-1}\left[\frac{\sin(-\beta_1)}{\mathrm{n}}\right]\right\}} \Bigg/ \cos\left\{\beta_2 + \sin^{-1}\left[\mathrm{n}\cdot\sin\left(\beta_1 - \beta_2 + \sin^{-1}\left(\frac{\sin(-\beta_1)}{\mathrm{n}}\right)\right)\right]\right\} \tag{5.14}$$

Now let us compare the results. Inputs are β_1=15,945°, β_2=8,13°, α_1=0°, D=40 mm and n=1,586. Our calculated outputs are $\Delta\alpha$=4,7036° and S=0,881 mm, outputs obtained from measurement in CATIA are in Figure 15, comparison of calculated and measured values is in Table 3.

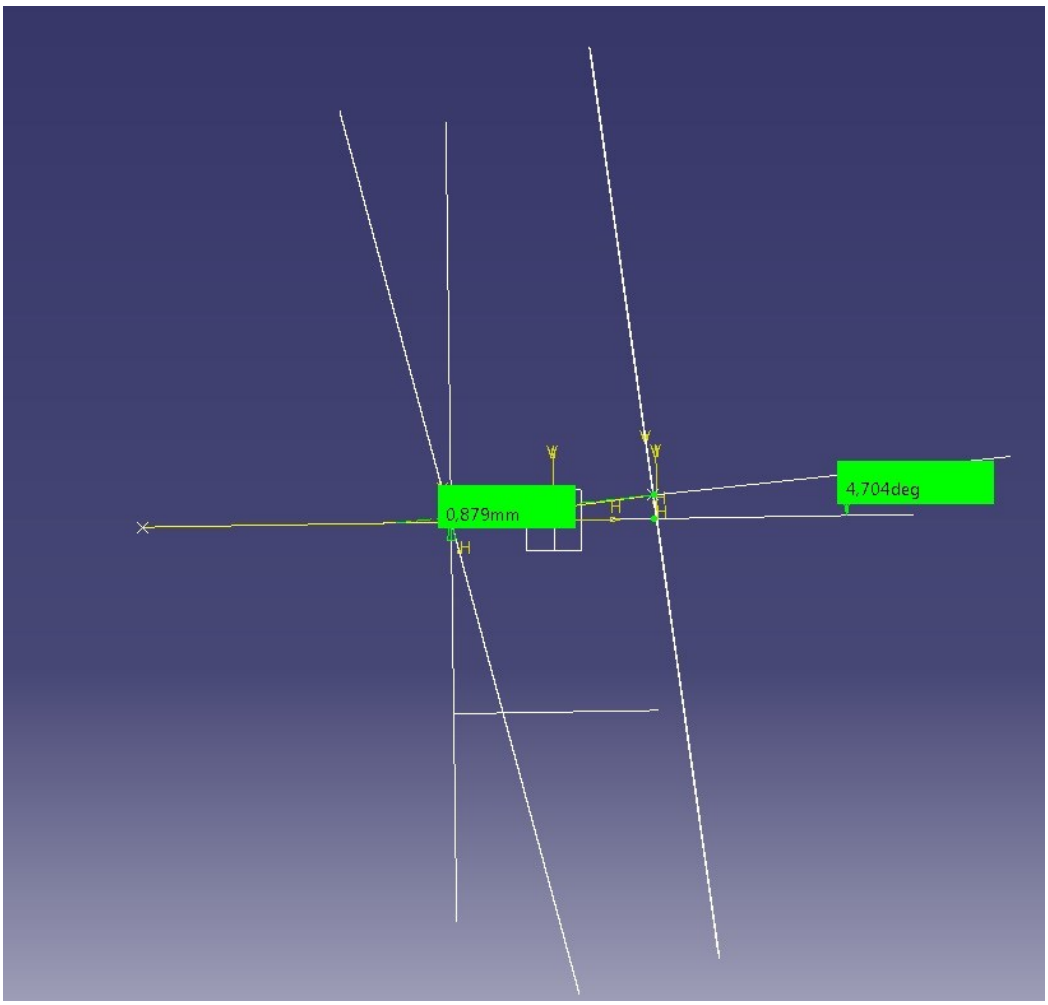

Figure 15: Values from CATIA in the second special case

The values match once again.

Table 3: Comparison of calculated and measured values

Values	Calculated	Measured
Deviation angle $\Delta\alpha$ [°]	4,7036	4,704
Beam shaft parameter S [mm]	0,881	0,879

Normal incidence

The third special case is the normal incidence, so $\alpha_1 = \beta_1$. Let us see how the formulas will vary:

$$\Delta\alpha = \beta_2 - \beta_1 + \sin^{-1}[n \cdot \sin(\beta_1 - \beta_2)], \tag{5.15}$$

$$S = \frac{\dfrac{D \cdot \cos\beta_2 \cdot \sin\{\beta_2 - \beta_1 + \sin^{-1}[n \cdot \sin(\beta_1 - \beta_2)]\}}{\cos(\beta_1 - \beta_2)}}{\cos\{\beta_2 + \sin^{-1}[n \cdot \sin(\beta_1 - \beta_2)]\}} \tag{5.16}$$

Regarding the results, inputs in this case are $\alpha_1 = \beta_1 = 15{,}945°$, $\beta_2 = 8{,}13°$, D=40 mm and n=1,586. Our calculated outputs are $\Delta\alpha = 4{,}64°$ and $S = 3{,}45$ mm, outputs obtained from measurement in CATIA are in Figure 16, comparison of calculated and measured values is in Table 4.

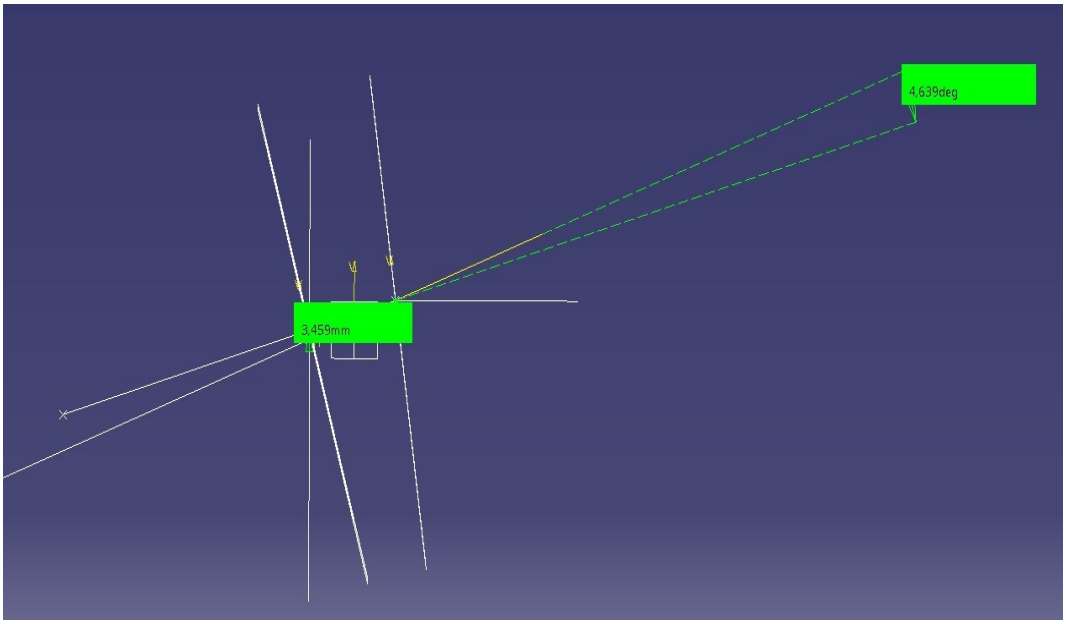

Figure 16: Values from CATIA in the third special case

As we can see, we have good compilance in our results.

Table 4: Comparison of calculated and measured values

Values	Calculated	Measured
Deviation angle $\Delta\alpha$ [°]	4,64	4,639
Beam shaft parameter S [mm]	3,45	3,459

Approximation of small angles

The last special case which we discuss is applying the approximation of small angles, as follows:

$$\sin\varphi \approx \varphi \,, \cos\varphi \approx 1 - \frac{1}{2}\varphi^2 \,. \tag{5.17}$$

With this approximation we obtain relations for our outputs:

$$\Delta\alpha \approx \beta_2 - \beta_1 + n \cdot (\beta_1 - \beta_2) \tag{5.18}$$

$$S \approx D \cdot \sin\left[\beta_2 - \beta_1 + \mathrm{n} \cdot (\beta_1 - \beta_2) + \alpha_1 - \beta_1 - \frac{\alpha_1 - \beta_1}{\mathrm{n}}\right] \tag{5.19}$$

We can apply approximation of small angles only to angles below 5°, so for our inputs we use these values: α_1=4,086°, β_1=2°, β_2=3°, D=40 mm and n=1,586. Our calculated outputs are $\Delta\alpha$≈0,586° and S≈0,1289 mm, outputs obtained from measurement in CATIA are in Figure 17, comparison of calculated and measured values is in Table 5.

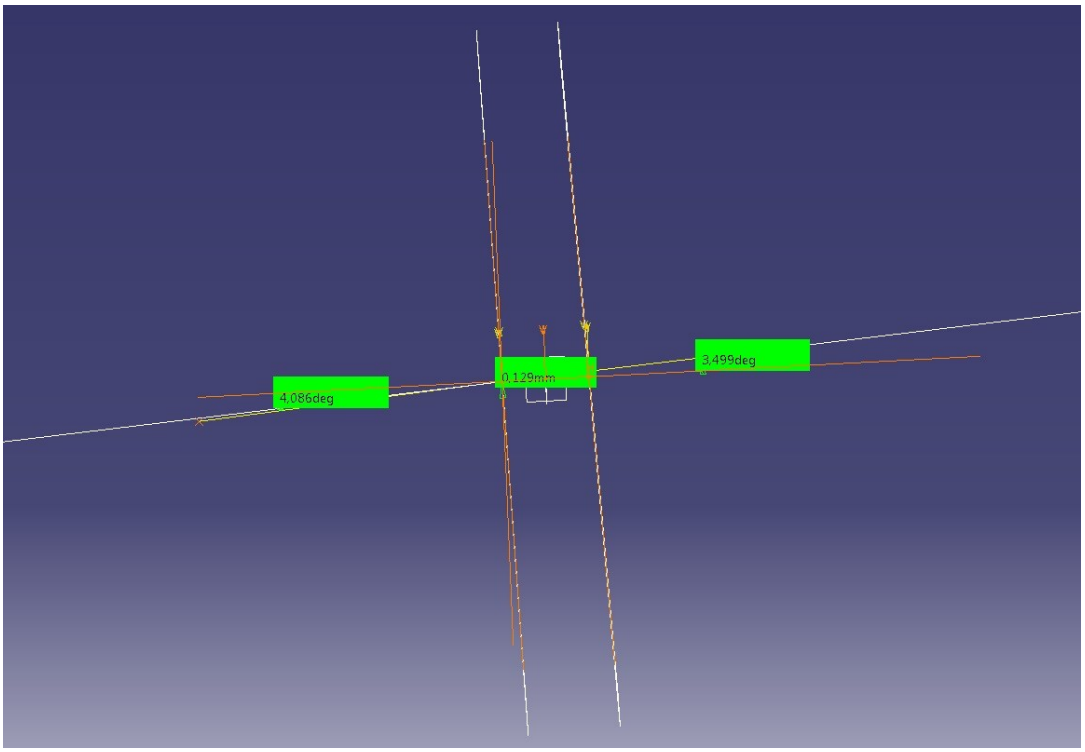

Figure 17: Values from CATIA in the fourth special case

Even in this case values match, so we can safely say, that our formulas are correct.

Table 5: Comparison of calculated and measured values

Values	Calculated	Measured
Deviation angle $\Delta\alpha$ [°]	0,586	0,587
Beam shaft parameter S [mm]	0,1289	0,129

5.2. Application of derived relations

The EXPOSE software, that will be used in the process of optimization, is creating neutral surface by modificating the inner surface of cover glass. In this modification the EXPOSE software uses parallel rays, which are incident on the outer surface of cover glass with angle of incidence α_1=0°. Because of that we use our derived relation (5.13) for view of dependence of the beam deviation angle $\Delta\alpha$ on angle $\Delta\beta$, which is the difference between angles of outer and inner surface, β_1 and β_2. Figure 18 shows this dependence.

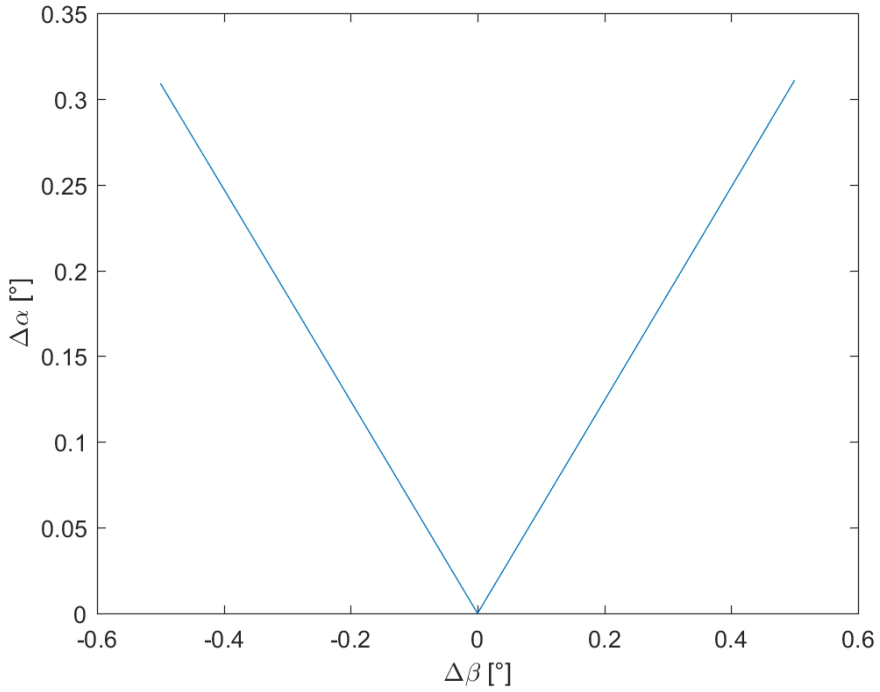

Figure 18: Dependence of the beam deviation angle $\Delta\alpha$ on angle $\Delta\beta$

For cover glass optical properties is very important that the beam deviation angle $\Delta\alpha$ has value lower than 0,3°, so from Figure 15 we can clearly see that difference between angles of outer and inner surface β_1 and β_2 must be lower than 0,5°. This information will be useful in the process of creating optimized cover glass.

5.3. Beam deviation on general surfaces

In this section we will briefly describe beam deviation on general surfaces. Section 5.1. showed how complicated are the relations for beam deviation angle in planar interface, so in this section we will only show how one could solve these issues in 3D-space. At first we move from planar interfaces to vector description with 3 coordinates, scheme is shown in Figure 19.

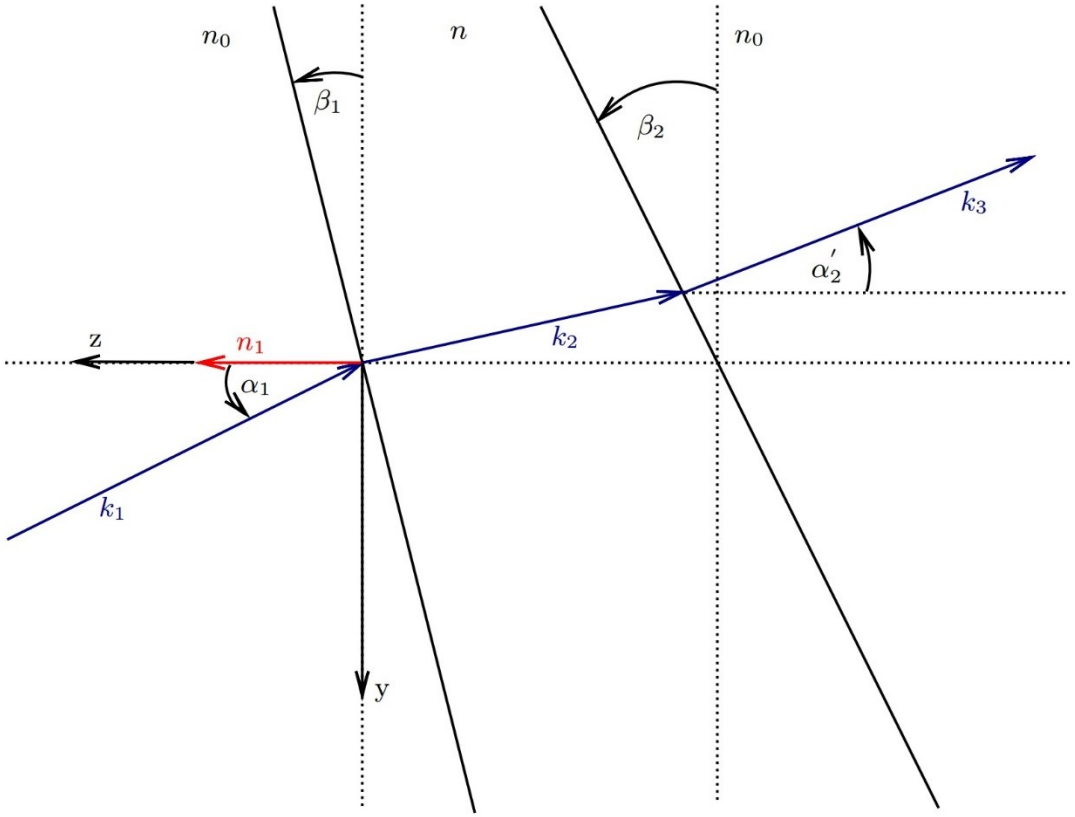

Figure 19: Representation of vectors

We are assuming that the wave is incident in *y-z* plane and therefore the normal vector $\mathbf{n_1}$ is derived as:

$$\mathbf{n_1} = (0; 0; 1), \tag{5.20}$$

and the vector $\mathbf{k_1}$ representing the incident ray:

$$\mathbf{k_1} = (0; \sin\alpha_1 ; \cos\alpha_1). \tag{5.21}$$

Now we must formulate the vector $\mathbf{k_3}$, representing the output ray:

$$\mathbf{k_3} = (0; \sin\alpha_2' ; \cos\alpha_2'), \tag{5.22}$$

where the angle α_2' is obtained using relations (5.1) – (5.5):

$$\alpha_2' = \beta_2 + \sin^{-1}\left\{\mathrm{n}\cdot\sin\left[\beta_1 - \beta_2 + \sin^{-1}\left(\frac{\sin(\alpha_1-\beta_1)}{\mathrm{n}}\right)\right]\right\}. \tag{5.23}$$

Our desired angle $\Delta\alpha$ can be obtained from scalar product:

$$\Delta\alpha = \cos^{-1}(\mathbf{k_1}\cdot\mathbf{k_3}), \tag{5.24}$$

from that we can get the final formula:

$$\Delta\alpha = \cos^{-1}(\sin\alpha_1\cdot\sin\alpha_2' + \cos\alpha_1\cdot\cos\alpha_2'). \tag{5.25}$$

A different approach is using the vectors defined by coordinates, scheme is shown in Figure 20. There is a different coordinate system, this one corresponds to a system which is used in optimization software.

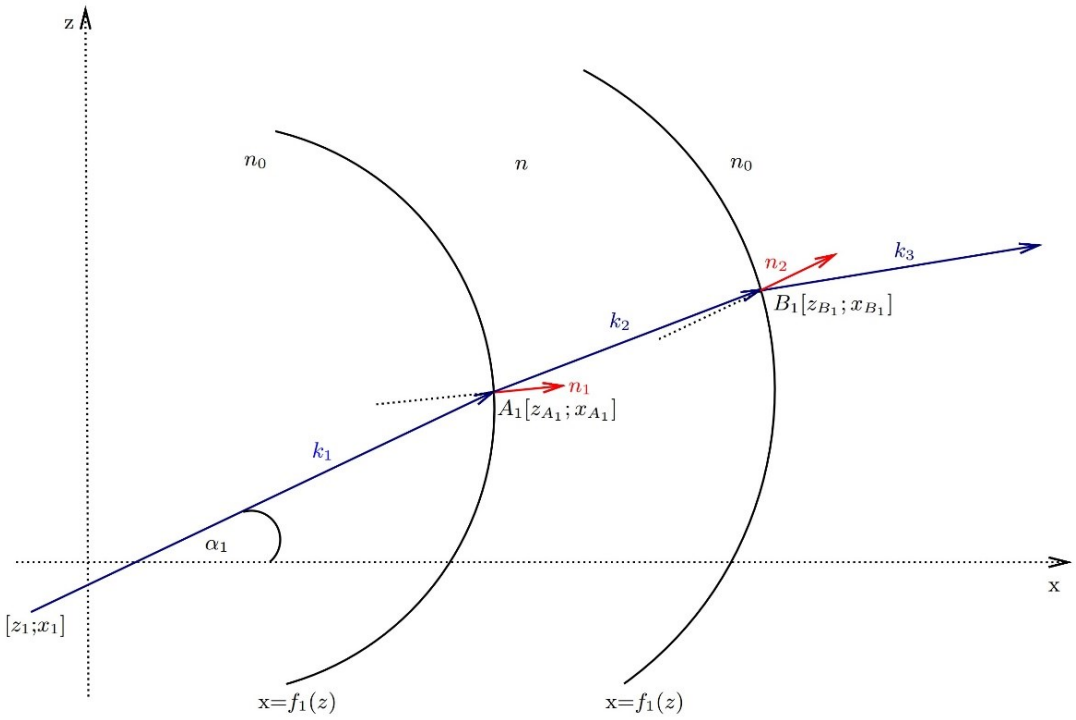

Figure 20: Representation of vectors defined by coordinates

Vector $\mathbf{k_1}$ representing the incident ray is defined in a same form as in the first case:

$$\mathbf{k_1} = (\cos\alpha_1\,; 0; \sin\alpha_1), \tag{5.26}$$

but in this case, we will use the parametric formula of line of this vector using coordinates:

$$z = z_1 + p\cdot\sin\alpha_1, \tag{5.27}$$

$$x = x_1 + p\cdot\cos\alpha_1. \tag{5.28}$$

After expressing the parameter p, we obtain equation of the line:

$$x = x_1 + (z - z_1)\cot\alpha_1. \tag{5.29}$$

Intersection point of line of vector $\mathbf{k_1}$ and surface $x=f_1(z)$ is point A_1 with coordinates $[z_{A1};x_{A1}]$. Using this point and derivation of surface we get formula of line in form:

$$x = x_{A1} + (z - z_{A1})\frac{\partial f_1}{\partial z}, \tag{5.30}$$

and from this formula we obtain normal vector $\mathbf{n_1}$:

$$\mathbf{n_1} = \left(1; 0; -\frac{\partial f_1}{\partial y}\right). \tag{5.31}$$

Now we need to obtain formula of vector $\mathbf{k_2}$, and we will get that using tangential and normal components of vectors, as it is shown in Figure 21.

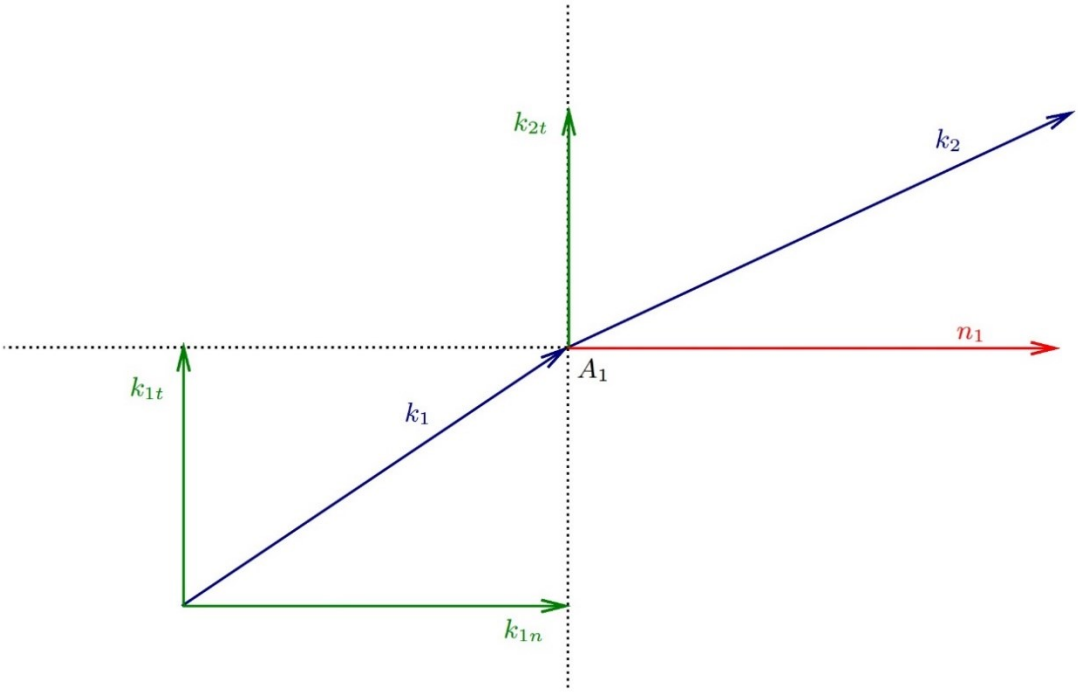

Figure 21: Tangential and normal components of vectors

Normal component of vector $\mathbf{k_1}$ is defined as:

$$\mathbf{k_{1n}} = \frac{(\mathbf{k_1}\cdot\mathbf{n_1})\mathbf{n_1}}{|\mathbf{n_1}|^2}. \tag{5.32}$$

Tangential component is obtained from normal component:

$$\mathbf{k_{1t}} = \mathbf{k_1} - \mathbf{k_{1n}}. \tag{5.33}$$

From the fact that the tangential components are preserved, we know that:

$$\mathbf{k_{1t}} = \mathbf{k_{2t}}. \tag{5.34}$$

Normal component of vector $\mathbf{k_2}$ can be defined as:

$$\mathbf{k_{2n}} = \chi \cdot \mathbf{n_1}. \tag{5.35}$$

where χ is parameter of displacement. We know that size of vector $\mathbf{k_2}$ is dependent on refractive index, therefore we have formula:

$$k_{2x}{}^2 + k_{2y}{}^2 + k_{2z}{}^2 = \mathrm{n}, \tag{5.36}$$

where in our case is k_{2y}=0. We can get parameter χ from components of vector $\mathbf{k_2}$:

$$k_{2x} = k_{2tx} + \chi \cdot n_{1x}\ , \tag{5.37}$$

$$k_{2z} = k_{2tz} + \chi \cdot n_{1z}\ . \tag{5.38}$$

So finally we can obtain vector $\mathbf{k_2}$ from relation:

$$\mathbf{k_2} = \mathbf{k_{1t}} + \chi \cdot \mathbf{n_1}, \tag{5.39}$$

where parameter χ is in form:

$$\chi = \frac{-2(k_{2tx}n_{1x}+k_{2tz}n_{1z}) \pm 2\sqrt{2k_{2tx}n_{1x}k_{2tz}n_{1z} - k_{2tz}{}^2 n_{1x}{}^2 - k_{2tx}{}^2 n_{1z}{}^2 + \mathrm{n}\cdot n_{1x}{}^2 + \mathrm{n}\cdot n_{1z}{}^2}}{2(n_{1x}{}^2 + n_{1z}{}^2)}. \tag{5.40}$$

When we apply the same method from (5.32) to (5.39) on vector $\mathbf{k_2}$ as an incident vector in second refraction, we can finally get output vector $\mathbf{k_3}$.

In this section we have shown how complicated can the description of light rays in cover glass for 3 dimensions be and with the knowledge that we got we are going to describe optics of real cover glass, which will be very important for our later optimization of cover glass.

5.4. Optics of real cover glass

In this section we will apply our relations on cover glass with a real shape. At first we will discuss the reflectance of glass and after that we will analyze beam deviation.

5.4.1. Reflectance of real cover glass

Each glass, no matter how transparent it is, has a considerable value of reflectance. Therefore we need to know what is the exact value of reflectance of polycarbonate (PC) glass, the material of cover glass that we will later analyze and use. We will calculate reflectance of our cover glass by reflection coefficients from Fresnel relations:

$$r_{\mathrm{s}} = \frac{n_1 \cos\theta_i - n_2 \cos\theta_t}{n_1 \cos\theta_i + n_2 \cos\theta_t}\,, \tag{5.41}$$

$$r_{\mathrm{p}} = \frac{n_2 \cos\theta_i - n_1 \cos\theta_t}{n_1 \cos\theta_t + n_2 \cos\theta_i}\,. \tag{5.42}$$

We obtain reflectances for *s*- and *p*-polarizations from these coefficients using the relations:

$$R_{\mathrm{s}} = |r_{\mathrm{s}}|^2\,, \tag{5.43}$$

$$R_{\mathrm{p}} = |r_{\mathrm{p}}|^2\,. \tag{5.44}$$

From these reflectances we are able to get total reflectance of material with relation:

$$R = \frac{1}{2}\left(R_{\mathrm{s}} + R_{\mathrm{p}}\right). \tag{5.45}$$

At this point we will apply relations (5.41) – (5.45) on the example of real cover glass, indices of refraction n_1 =1 (air), n_2=1,586 (PC). The scheme of both refractions with incident and transmission angles is shown in Figure 22.

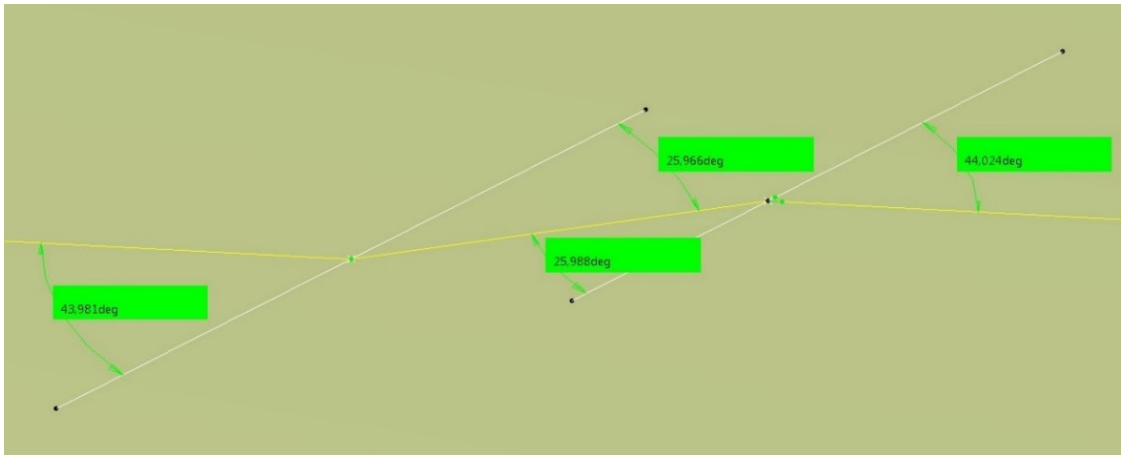

Figure 22: Incident and transmission angles on real cover glass

From Figure 19 we can see that for the first refraction the incident angle θ_i has the value of 43,981° and transmission angle θ_t of 25,966°. From relations (5.41) – (5.44) we obtain reflectances R_s=0,108 and R_p=0,014 and from relation (5.45) the total reflectance for first refraction R=0,061. Using this method for second refraction we get total reflectance for second refraction R=0,0615. We can see that for each interface around 6,1% of rays will reflect back and that is quite a significant value that we need to take into consideration.

5.4.2. Beam deviation of real cover glass

Let us try our calculations with real glass from car lighting which we will later optimize. We will take inner and outer surface of this glass and calculate the refraction using relations (5.8) and (5.10) and let us find out if we can calculate it correctly. For our inputs we use these values: α_1=8,25°, β_1=27,12°, β_2=27,152°, D=3 mm and n=1,586. Our calculated output is $\Delta\alpha\approx$0,021°, output obtained from measurement in CATIA is $\Delta\alpha\approx$0,024° and the whole scheme is in Figure 23, the comparison of outputs is in Table 6. We can see that there is a little difference in outputs, but it can be caused by angles β_1 and β_2, which are difficult to determine in these curved surfaces and we obtained them from tangential planes on our incident points.

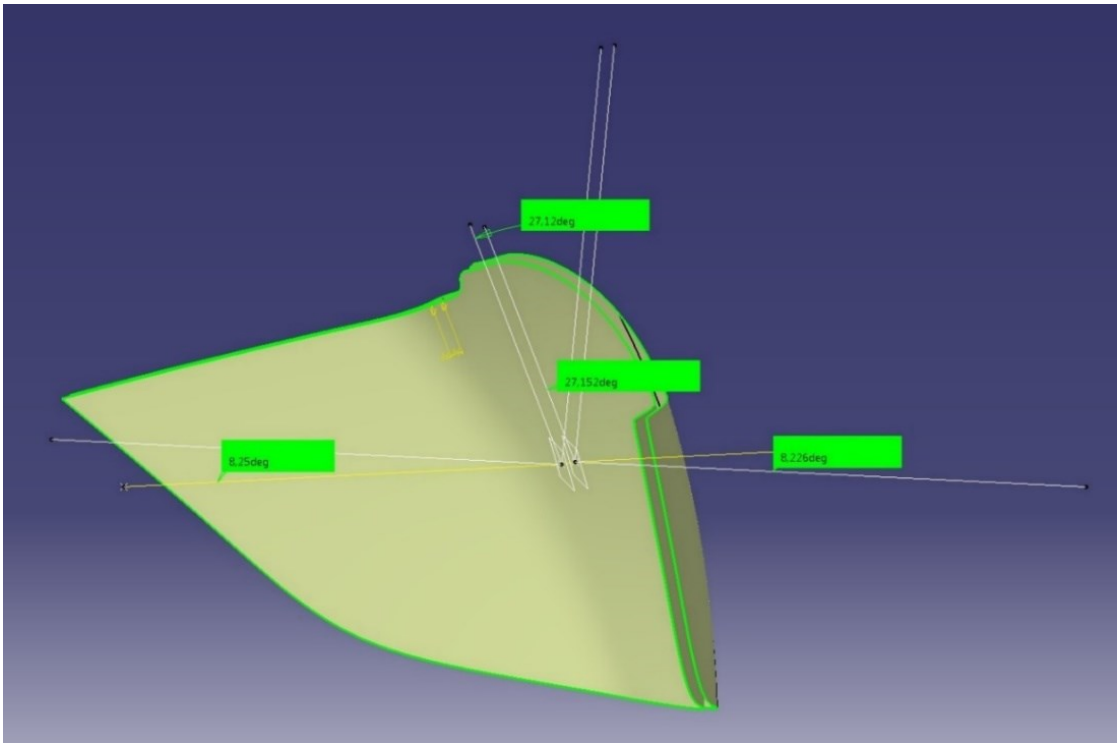

Figure 23: Refraction of ray on real glass in car lighting

Table 6: Comparison of calculated and measured value

Values	Calculated	Measured
Deviation angle $\Delta\alpha$ [°]	0,021	0,024

At this time when we understand the refraction of rays in two surfaces we can start optimizing the real cover glasses used in automotive industry. The motivation is to create an optimized glass which minimalizes the ray deviation but is not hard for manufacture and it has fine viewing properties. Figure 24 shows how the rays refract in a regular cover glass.

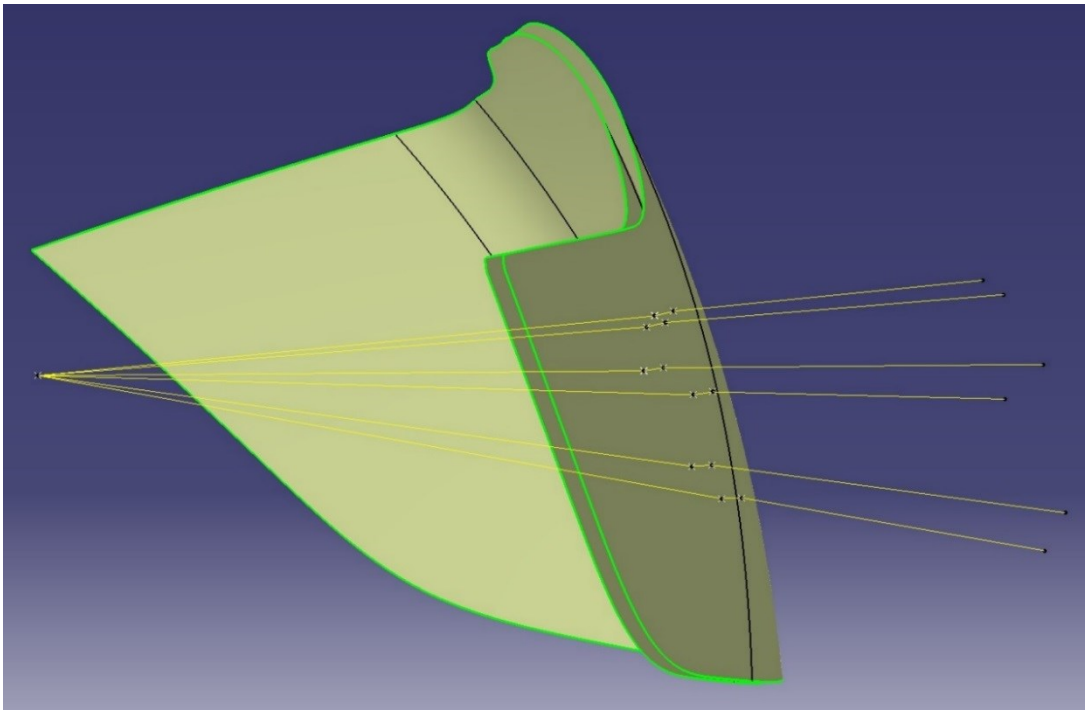

Figure 24: Refraction of multiple rays on real glass in car lighting

We can see the slight refractions and it is our goal now to minimalize deviations of input and output rays. Let us start with the optimization in EXPOSE software, which was developed in Varroc Lighting Systems, s.r.o. This software modify the inner surface of the glass, the outer surface is unchanging.

During the process of optimization, EXPOSE software is using parallel rays, which impact on the outer surface and based on the Snell's law of refraction creating the new inner surface which minimalizes deviation of these rays. When we have unoptimized glass, the normal of surface around incident point is different than the normal of surface around output point of refracted ray. EXPOSE software is creating the optimized inner surface which minimalizes these differences in normals of inner and outer surfaces.

6. Optimization of cover glass of headlamp using software

This chapter contains optimization of cover glass using software, commercial and software created in Varroc Lighting Systems, s.r.o. At first, we discuss manufactory of cover glass, then there is the main part of this thesis concerning whole optimization and in the end of this chapter there are shown results of our developed method. Optimization of cover glass contains multiple steps, which some of them require quite a skill. In the first part of this chapter is a guideline for optimization using software CATIA and EXPOSE, then there is an analysis made with software LucidShape, LuxRender, LightTools and Beam Analyzer, and in the end the results of our process of optimization are shown, and also a different method for optimization. Let us guide you through the whole process.

6.1. Manufactory limits of cover glass

We could create perfectly optimized cover glass regarding beam deviation if we would not be limited by manufactory limits of cover glass, but because there are a few manufactory limits resulting from production procedure, we must follow some rules. The general rule is that common thickness of cover glass is around 3 mm, in minimum we can go up to 2,5 mm and in maximum up to 4,5 mm, therefore we follow these limits in our parameters of optimization. These limits are necessary to be respected because of several tests that are applied to each cover glass, for example temperature, chemical and impact tests. Another manufactory limit comes from place of influx in manufactory procedure, because cover glass from PC (mentioned in chapter 2.3.) is made from one place of injection. It is useful to know where this place on cover glass will be, because around the place of injection the cover glass is thicker and on the contrary in places far from the place of injection is the cover glass thinner. These two limits are most important to follow in a procedure of designing new cover glass and therefore we will follow them in our process of optimization.

6.2. Guideline for optimization of cover glass

In this chapter we create a guideline for process of optimization of cover glass, which will be available for employees of company Varroc Lighting Systems, s.r.o. to perform optimization of cover glass for any kind of headlamp. In the beginning of process of optimization, we modify the cover glass in CATIA software with a series of different steps and then the optimization in EXPOSE software starts which is crucial for this process.

6.2.1. Modifications in CATIA software

Let us start with the process. First step in CATIA is extracting the cover glass from a whole reflector, which is shown in Figure 25.

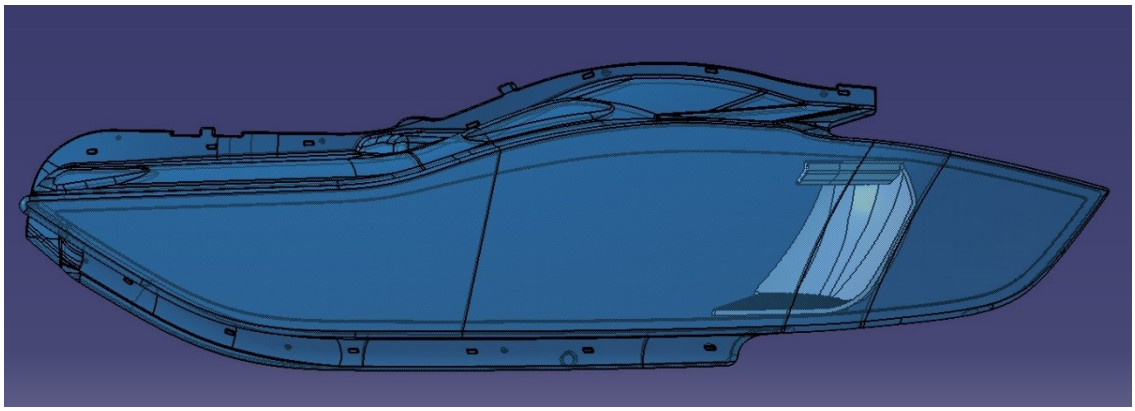

Figure 25: Initial part

For extracting the glass, we use the function Multiple extract and we pick the right parts. It is also important to choose some parts of Kink reflector, which is the reflector for low beam function of headlight, as it will be explained later.

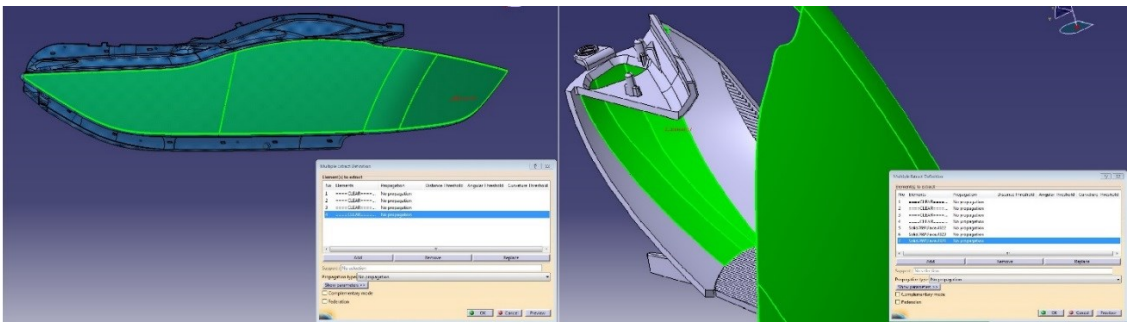

Figure 26: Extracting the right parts

After we extract the right parts then it is important to choose some point on surface from Kink reflector, which indicates position of light source, which is crucial for optimization and analysis. Both steps are shown in Figures 26 and 27.

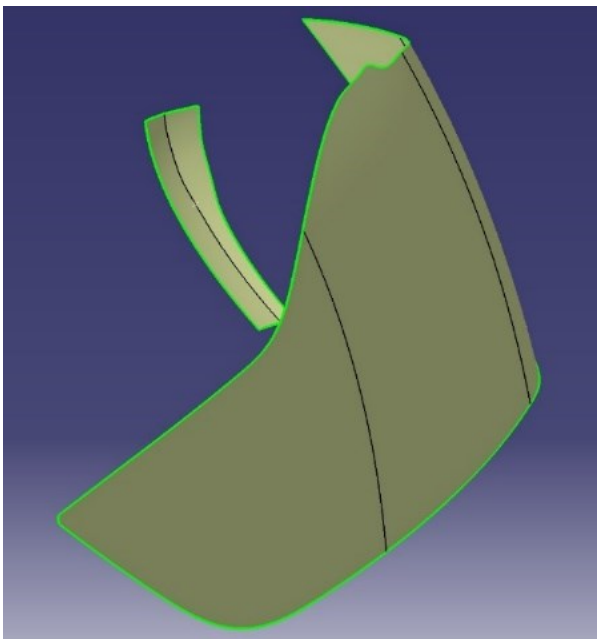

Figure 27: Extracted parts with point indicating the source of light

Next step is creating axis system in this point and using the function Axis to axis we translate our glass to Absolute axis system. Because the reflector is originally oriented in $-x$ axis, we need to rotate it alongside the z-axis by 180°. Figure 28 shows this operation.

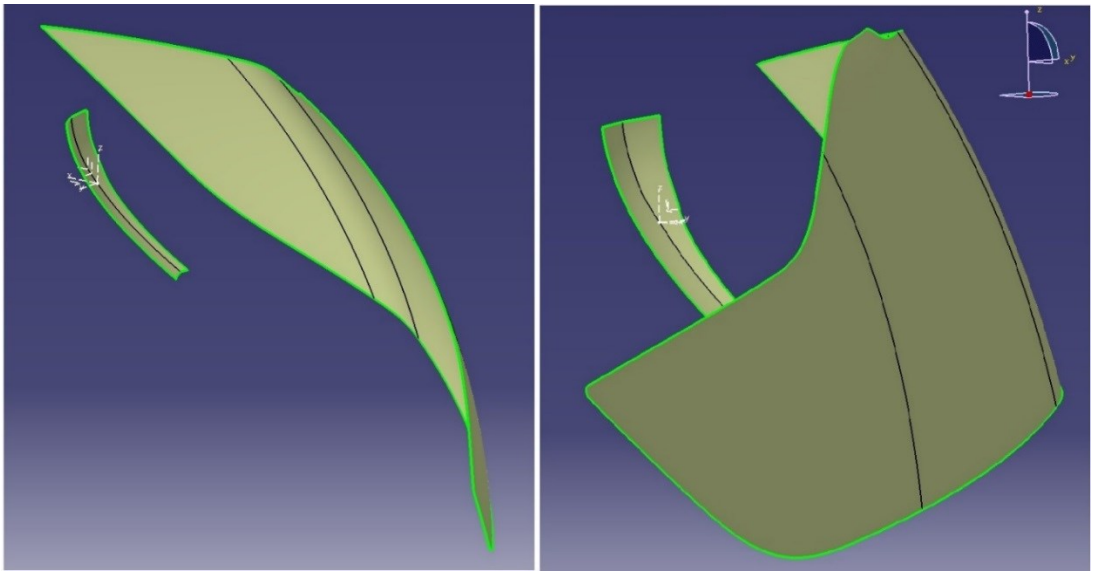

Figure 28: Translation and rotation of extracted parts

At this point we are ready to optimize the cover glass using EXPOSE software, but we will make some adjustions to make it run smoother. Using the function Multiple extract we choose the parts containing glass only, then we join these parts using the function Join and create a line of the edge of glass using the function Boundary, as it is displayed in Figure 29.

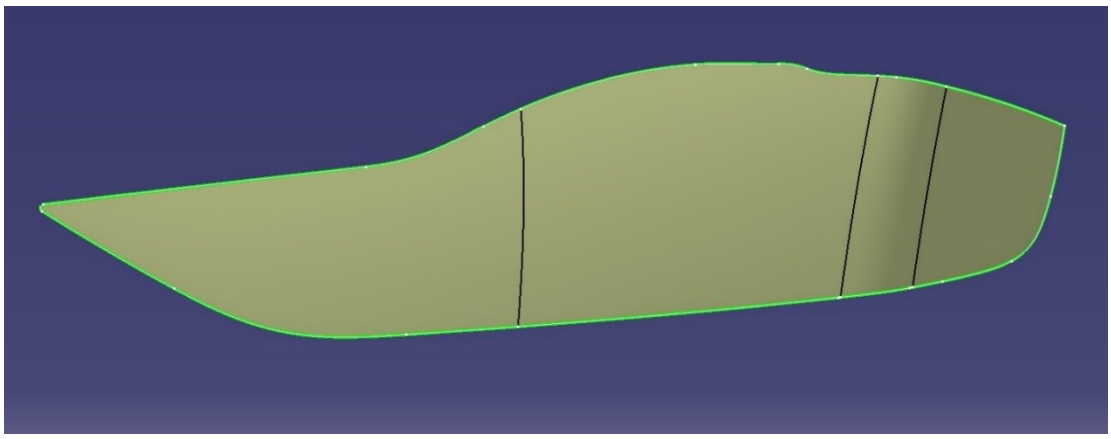

Figure 29: Joined parts of glass with shown boundary

If we try optimizing this surface in EXPOSE we would get some result, but the software would probably shrink the surface, which is an unwanted effect. So, to avoid this we extrapolate our surface. Either we extrapolate whole surface, or we use the function Disassemble and we extrapolate each surface individually, as it is shown in Figure 30. The second option is more frequent because of CATIA software functioning. When we extrapolate parts separately, then it is useful to join these parts subsequently. It is not possible in every case.

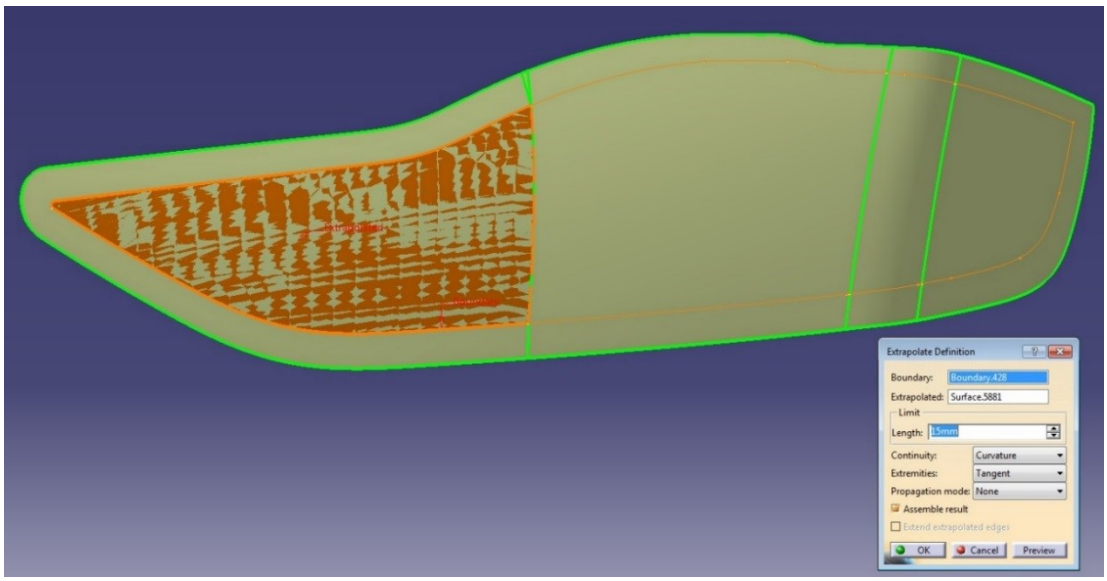

Figure 30: Extrapolating the original surface

We are now ready for optimization in EXPOSE software. We need to have two exact surfaces, indicating outer glass (A – surface) and inner glass (B – surface) offseted from each other. So for example we choose that our extrapolated surface is outer glass and we use function Offset and we move it with direction to the inside with required distance, usually about 3 mm as it is shown in Figure 31.

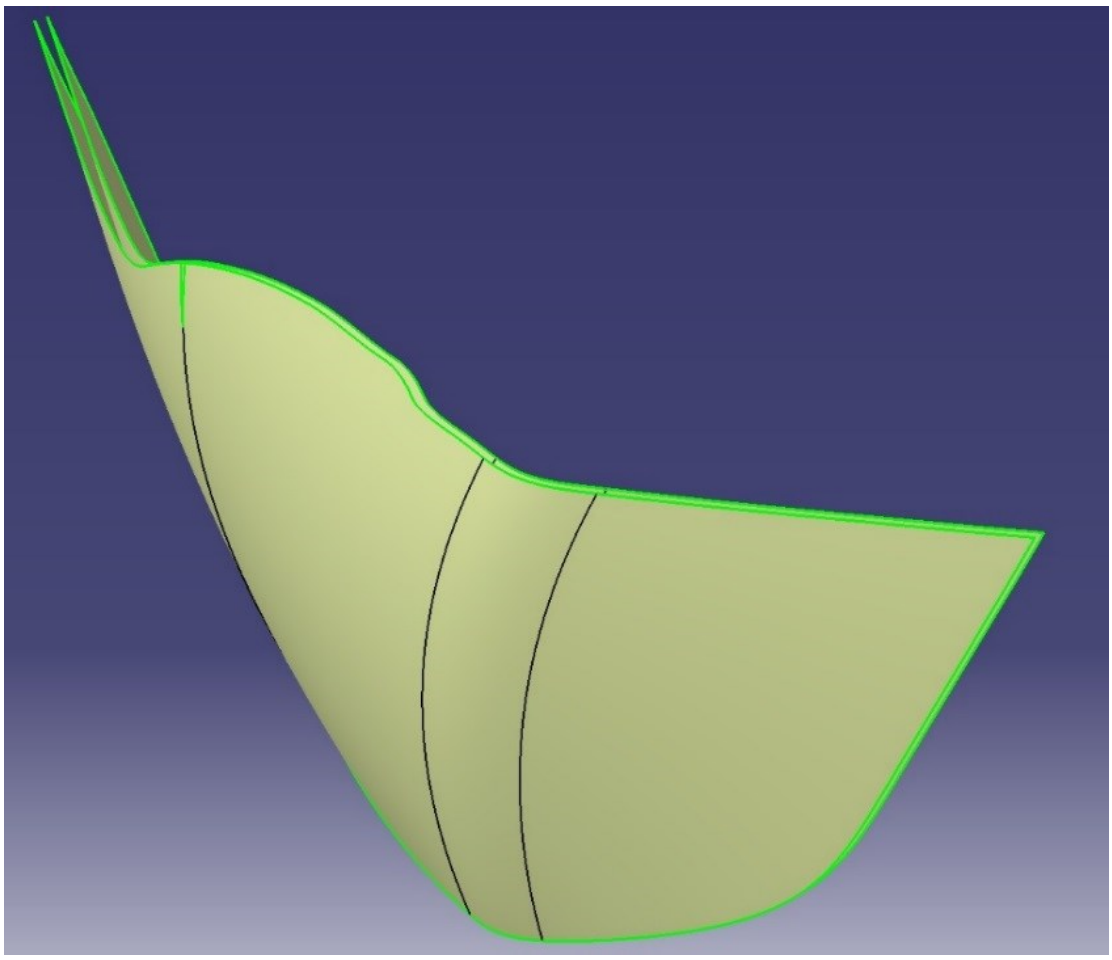

Figure 31: Outer and inner surface of our glass

6.2.2. Optimization in EXPOSE software

EXPOSE software operates with outer and inner surface separately, so it is necessary to save each surface to its own IGS file, for example A.igs and B.igs. We save both these files to a new folder in EXPOSE folders and we create an .edi file, which is associated with EXPOSE software and we can modify it with notepad. The specific settings and interface of EXPOSE software is a property of Varroc Lighting Systems, s.r.o. and therefore it is not included in this thesis.

When we run the EXPOSE .edi file, the algorithm starts and it will take a while to complete the optimization. When the optimization is finished, the new IGS file is created with new inner surface from EXPOSE software. We can clearly see that the new surface is slightly deformated, Figure 32 shows new inner surface with boundary of original inner surface.

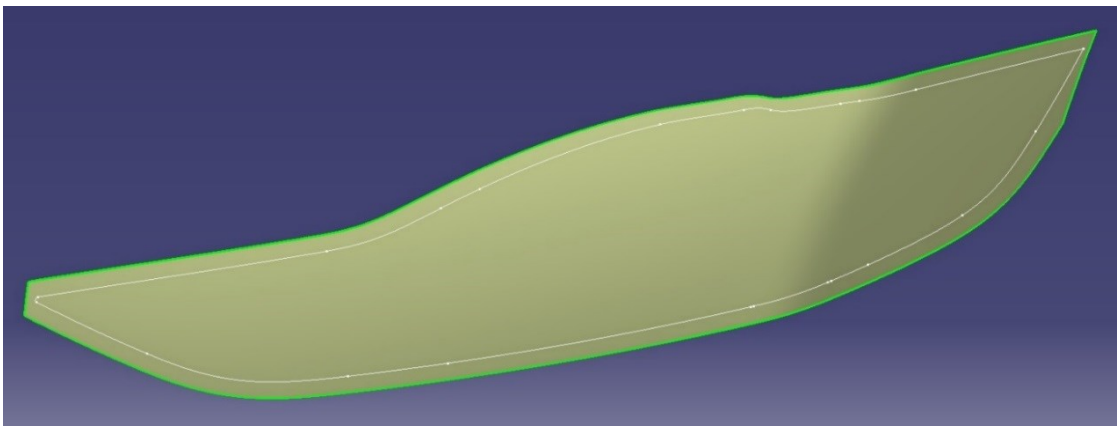

Figure 32: New inner surface from EXPOSE software

It is necessary for the new surface to be larger than original surface represented by the shown boundary. It often happens that the new surface does not cover the boundary in every point, so the original outer and inner surfaces need to be extrapolated more. It is kind of a trial and error method.

When the created surface is finally large enough then it is time to modify it, so it will have the same boundary as the original inner surface. For that we use function Extrude, which makes a surface from that boundary and then function Split for our desired optimized inner surface, Figure 33 shows this operation.

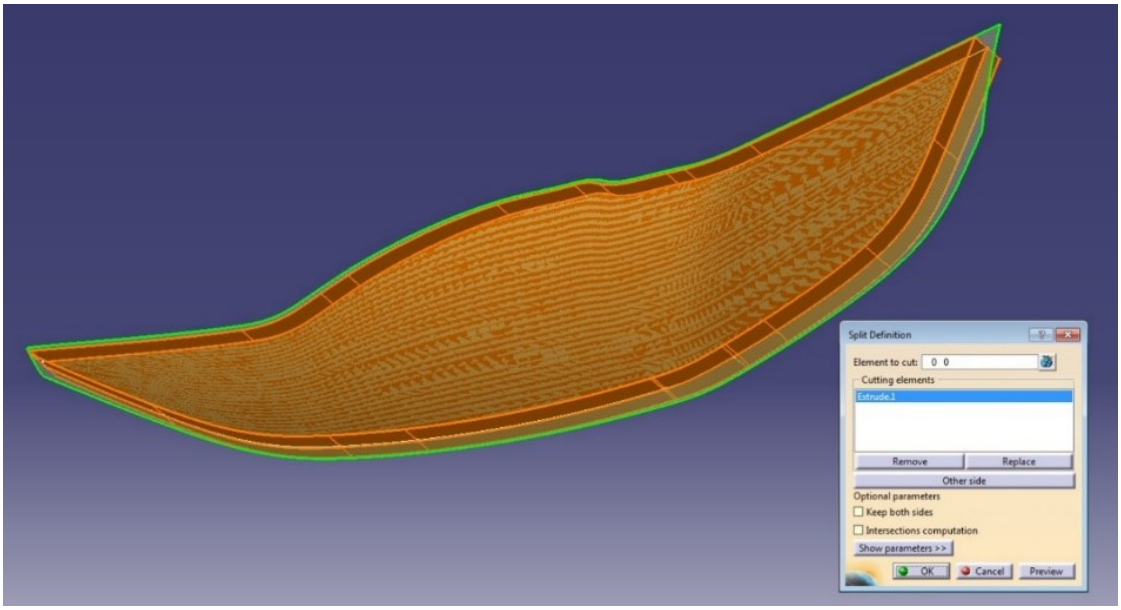

Figure 33: Obtaining the final optimized inner surface

6.2.3. Analysis of cover glass

At this point we have obtained our optimized glass and now it is time for analysis, but at first, we should understand how EXPOSE software operates and for this we use the function Wall Thickness Analysis in CATIA software. We need a special license for using this function and this license is called CCV - CORE & CAVITY DESIGN 2.

Figure 34: CCV license for Wall Thickness Analysis function

For using the function Wall Thickness Analysis, we must create a solid from our surface and then we find this function in Part Design in CATIA software. Figure 35 shows the wall thickness analysis of our optimized glass, we can see the differences in thickness but all within the range that we set.

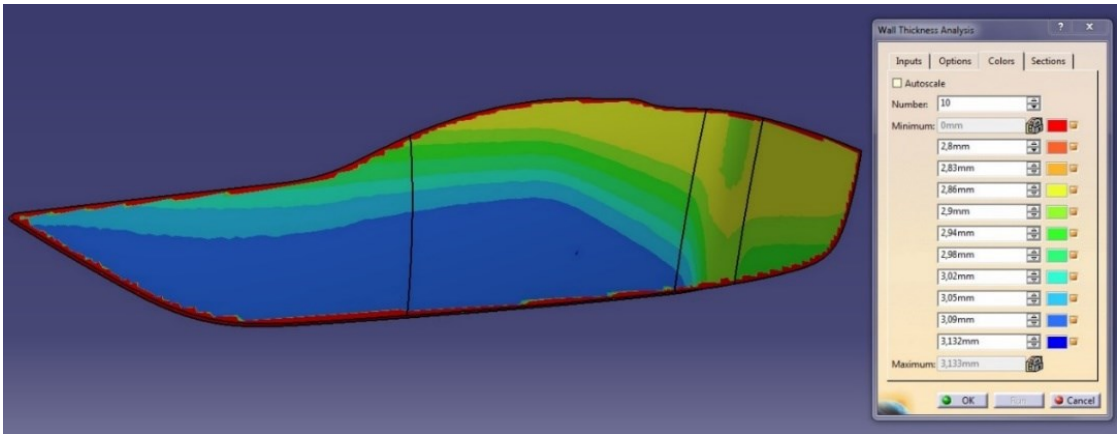

Figure 35: Wall thickness analysis of our optimized glass

For a purpose of analysis, we are using the LucidShape software. In CATIA software we put our original outer surface with created inner surface to one window, then we open LucidShape software and with function CATIA Transfer we transform our surfaces to LucidShape for analysis. We assign the material to surfaces, choose index of refraction 1,586 (same as for EXPOSE software) and start analysis with function Ray Deviation and Checkerboard Analysis. LucidShape uses different axis system, so we need to set analysis correctly as it is shown in Figure 36.

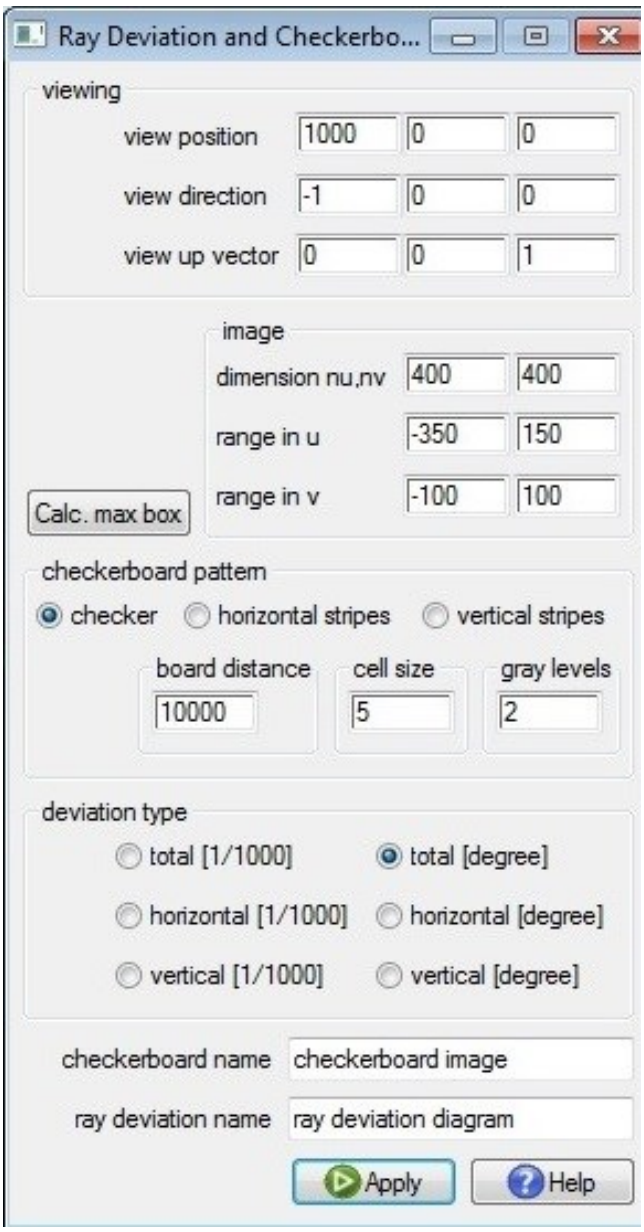

Figure 36: LucidShape settings

A little troublesome is setting of range, because LucidShape software does not provide any preview, so that is a trial and error method too. Once we set the appropriate range we start the analysis with deviation type of total [degree] and later horizontal [degree] and vertical [degree], subsequently. Now we have analysis of ray deviation of our glass, but we need to have something to compare with, so in CATIA software we take the original outer surface, offset it with the same distance as we did in optimization and then perform the same analysis. Comparison of total ray deviation of offseted surfaces and our optimazed surface is shown in Figure 37.

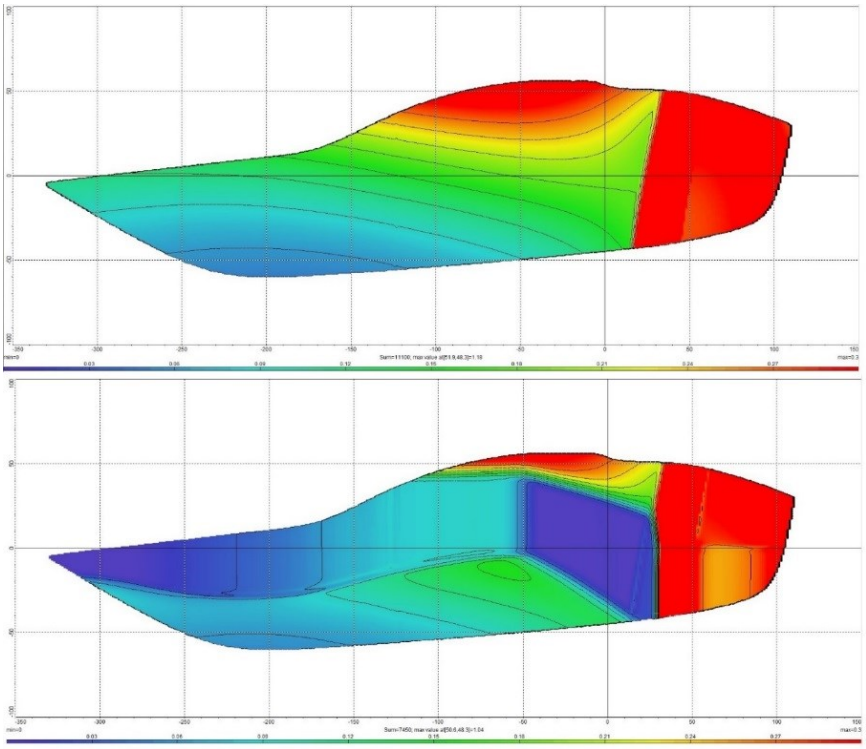

Figure 37: Comparison of total ray deviation

In our comparison we set the maximum deviation to value 0,3° which is represented by the red colour. On the upper part is glass with offseted outer surface, on the lower part is glass with our inner optimized surface. We can clearly see the improvement, especially around the area of light source. It is also interesting to separate horizontal and vertical deviations, these analyses are shown in Figures 38 and 39.

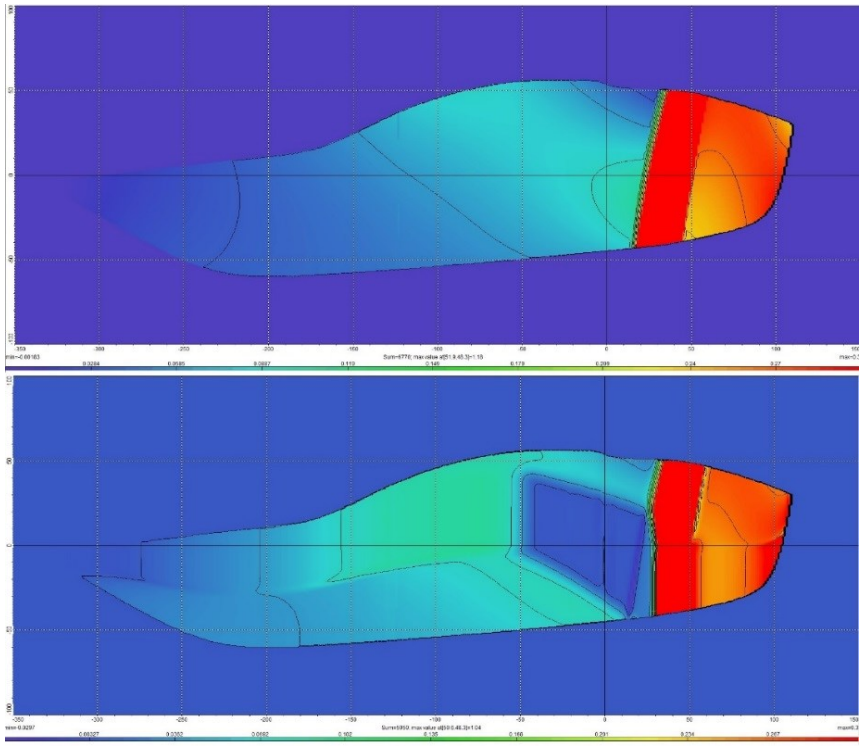

Figure 38: Comparison of horizontal ray deviation

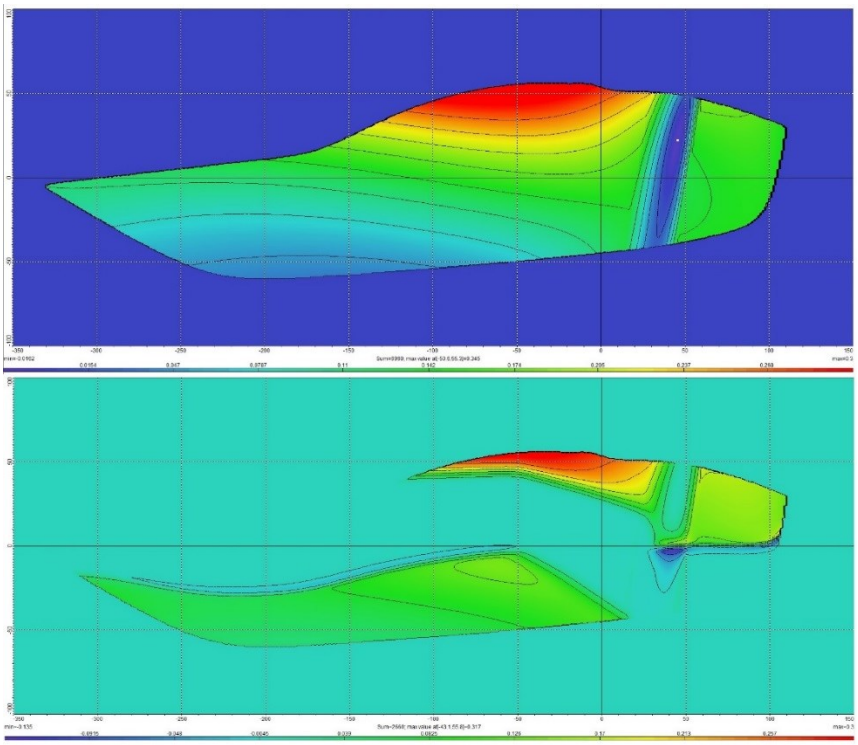

Figure 39: Comparison of vertical ray deviation

LucidShape software also provides checkerboard analysis which shows viewing properties of glass. This comparison is shown in Figure 40.

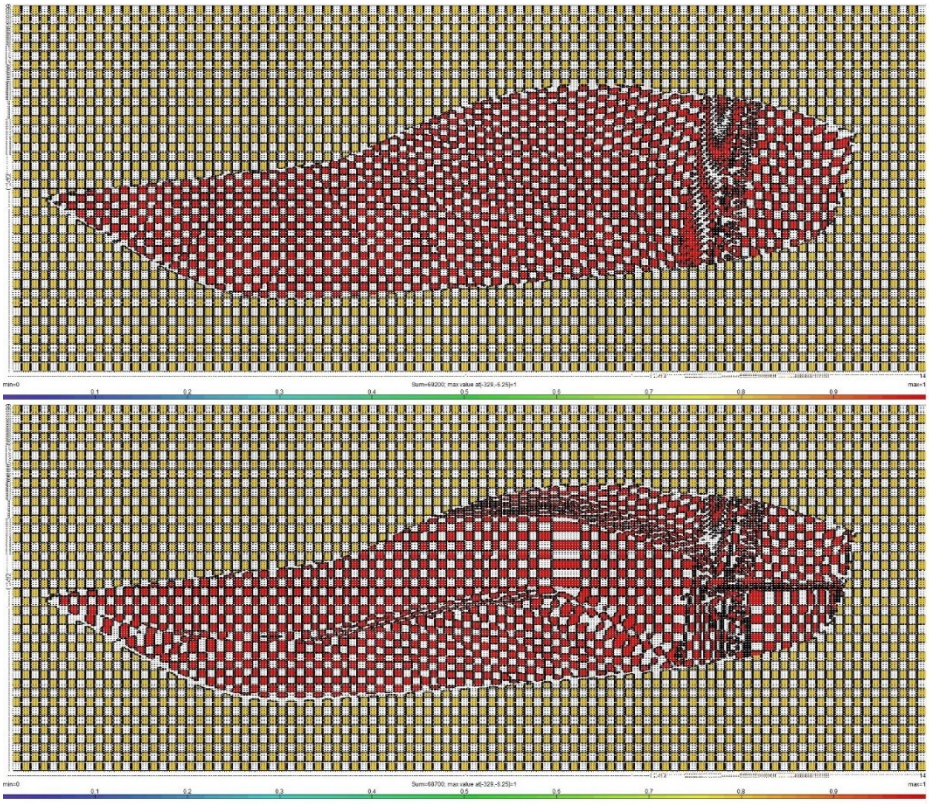

Figure 40: Comparison of checkerboard analysis

In this comparison the optimized glass seems to have worse viewing properties than the glass with offseted surfaces, but as it will be shown later, it is definitely not that bad

in a reality. For a realistic display of viewing properties we use the software LuxRender. We have created special background in CATIA software, from our surfaces created a solid and appropriately set in LuxRender software. Figures 41 and 42 show viewing properties of glass made of offseted surfaces and our optimized glass, separately.

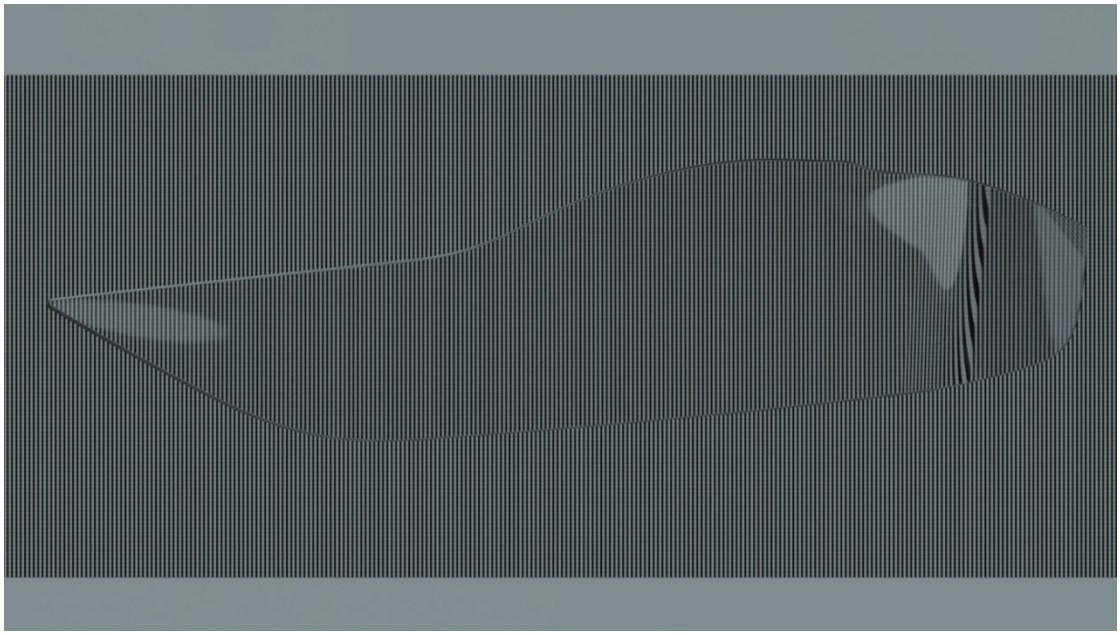

Figure 41: Viewing properties of glass made from parallel surfaces

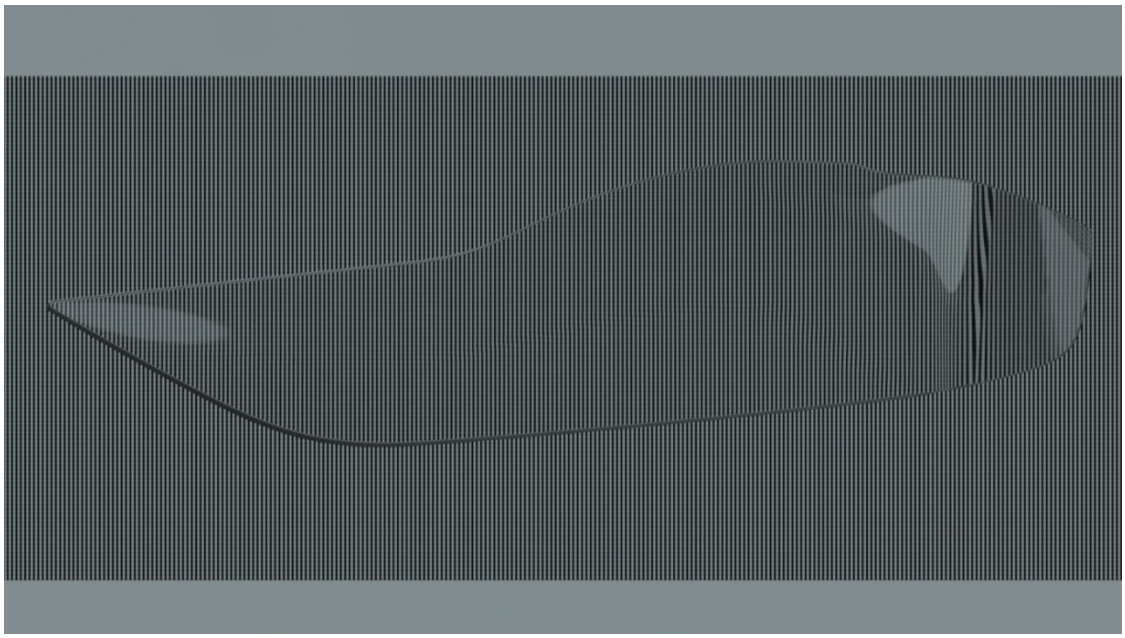

Figure 42: Viewing properties of optimized glass

This comparison shows us that our optimized glass doesn't have worse viewing properties than unoptimized glass, on the contrary it looks better and we can announce that we can create optimized glass with improved viewing properties. At this point we will make last analysis and that should be analysis of map of light intensity. For that purpose we use software Beam Analyzer, developed in Varroc Lighting Systems, s.r.o.

Figure 43 shows this analysis for projector unit with light source, specifically low beam function.

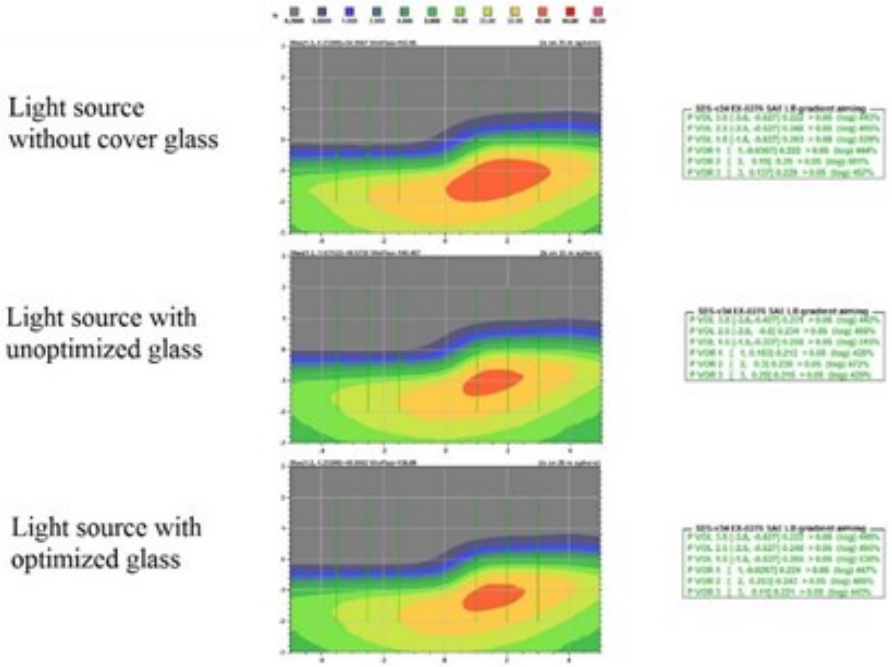

Figure 43: Analysis of map of gradient aim

On the top there is a map for light source without glass, in the middle is light source with unoptimized glass and on the bottom is light source with our optimized glass. The second and third map look very similar, but there are some important details of gradient aim (sharpness factor) in which they differ. In Figure 43 we can't see the coordinates properly, so in the detail in Figure 44 we highlighted the important columns.

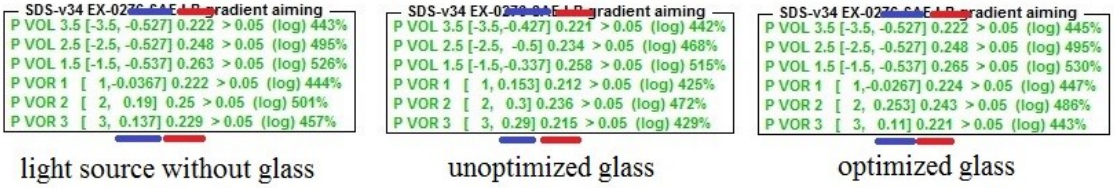

Figure 44: Important details of analysis

Blue marked columns show vertical positions of gradient, red marked columns show values of gradient, which is calculated from relation:

$$G = \log E_{\beta} - \log E_{(\beta+0,1°)}\ , \tag{5.1}$$

where β is horizontal value in degrees. Our goal is to have both these values as similar as in the case of light source without glass, and we can clearly see that our optimized glass exhibits much better results than unoptimized glass.

6.3. Difficulties in the process of optimization

From the previous results which are not bad at all we could announce that our method is applicable to optimization of cover glass, but the process of optimization is not that smooth in every case, as we are going to show now. When we tried optimizing a different glass with different shape, we obtained very different results. Figure 45 shows comparison of total ray deviation of offseted surfaces and our optimazed surface.

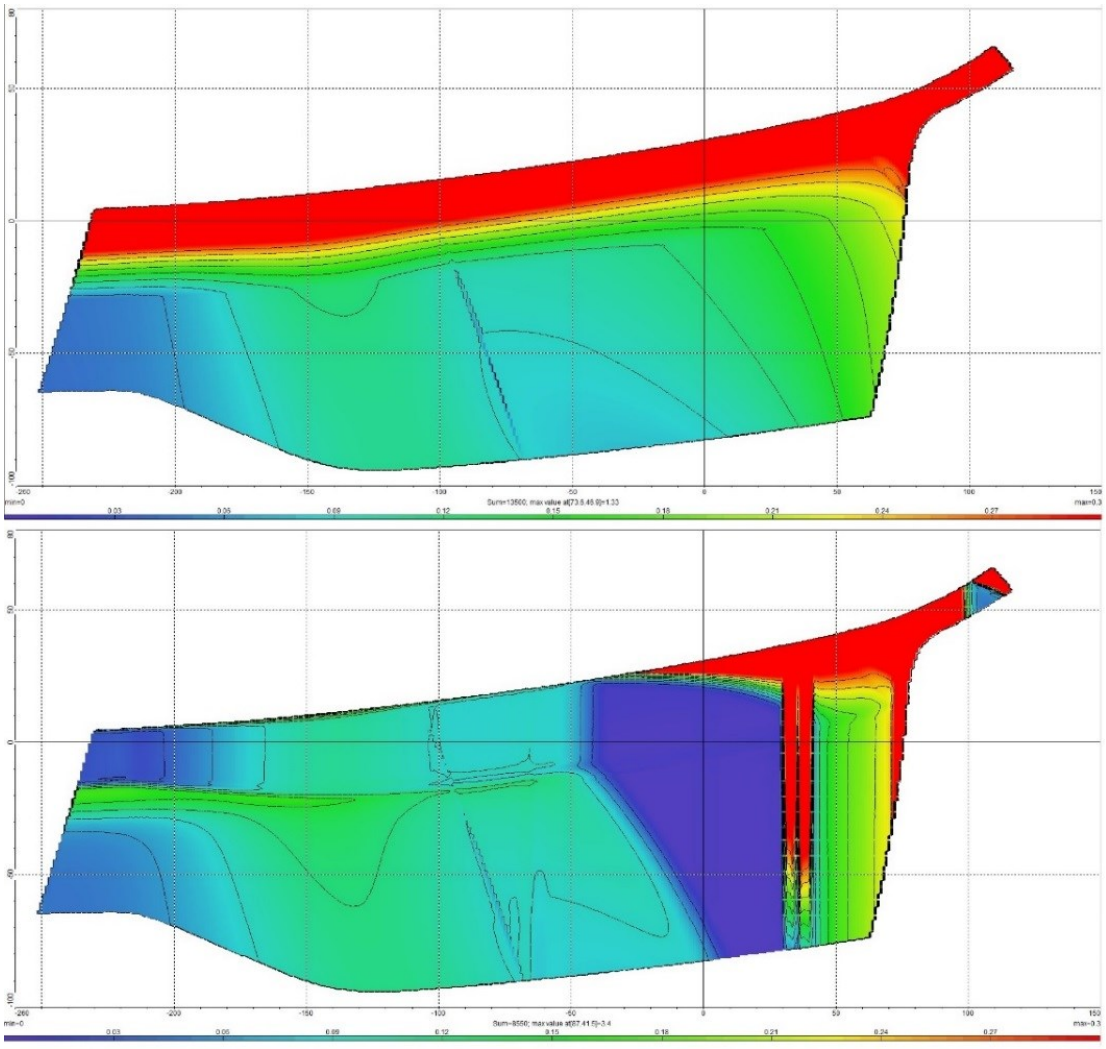

Figure 45: Comparison of total ray deviation

We can see a considerable improvement in our optimized surface, but there are much steeper changes than in case of offseted surfaces. Let us see how much this effect will influence viewing properties. Figures 46 and 47 show this analysis.

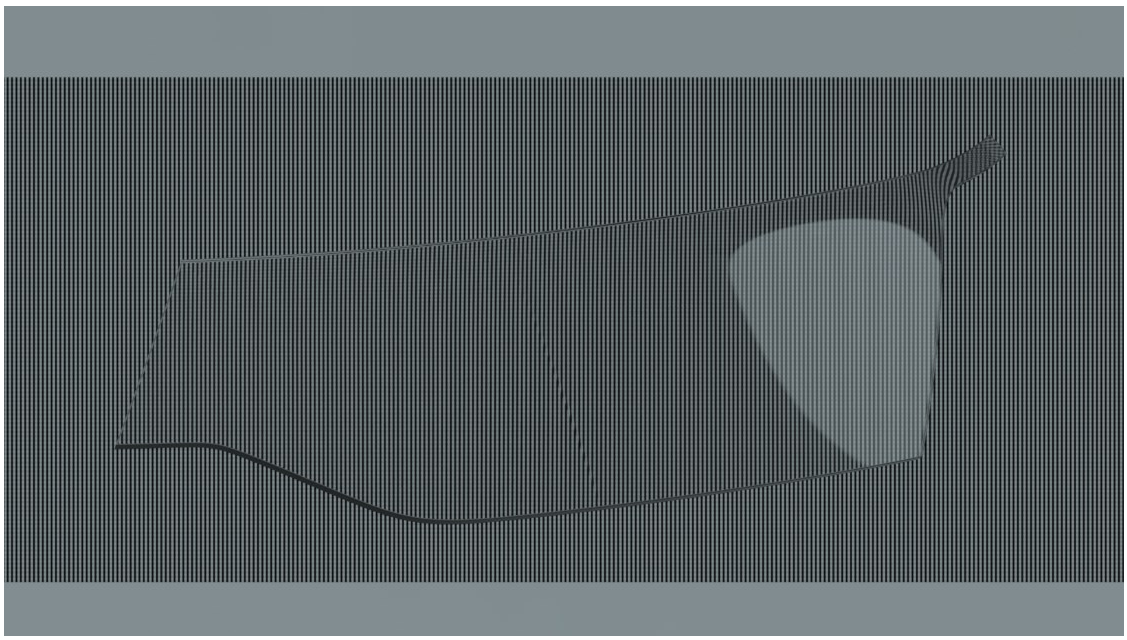

Figure 46: Viewing properties of glass made from parallel surfaces

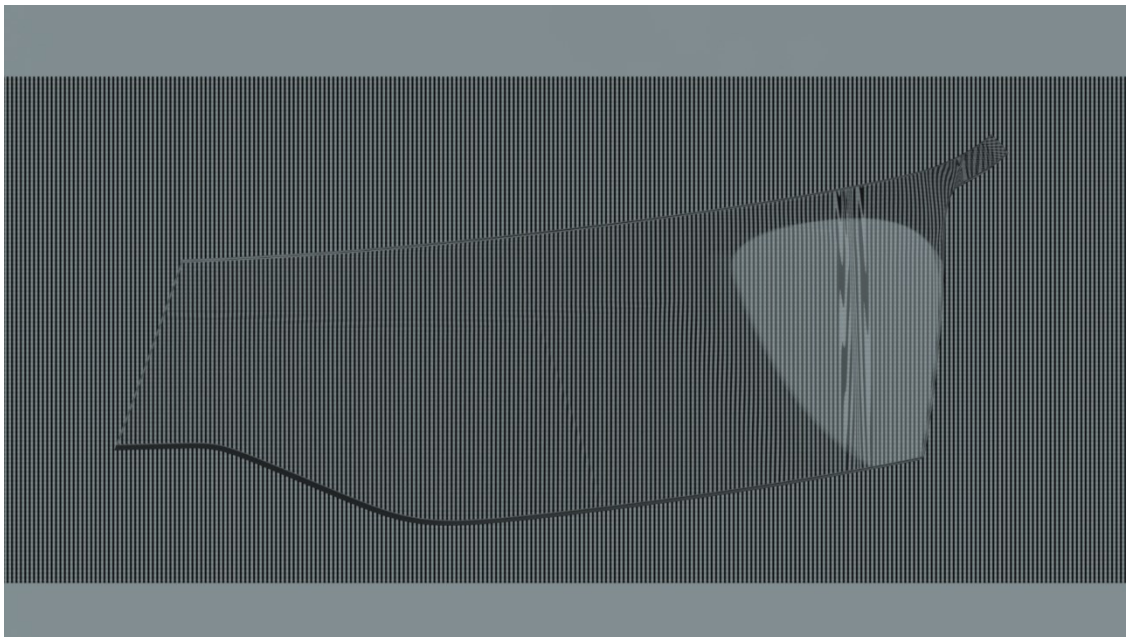

Figure 47: Viewing properties of optimized glass

We can notice obvious deffects in right side of glass which is unwanted effect. To avoid this we will try different settings of EXPOSE software and let us see if the results will be better, specific settings of the EXPOSE software can't be shown in this thesis, results of the new settings are shown in Figures 48 and 49.

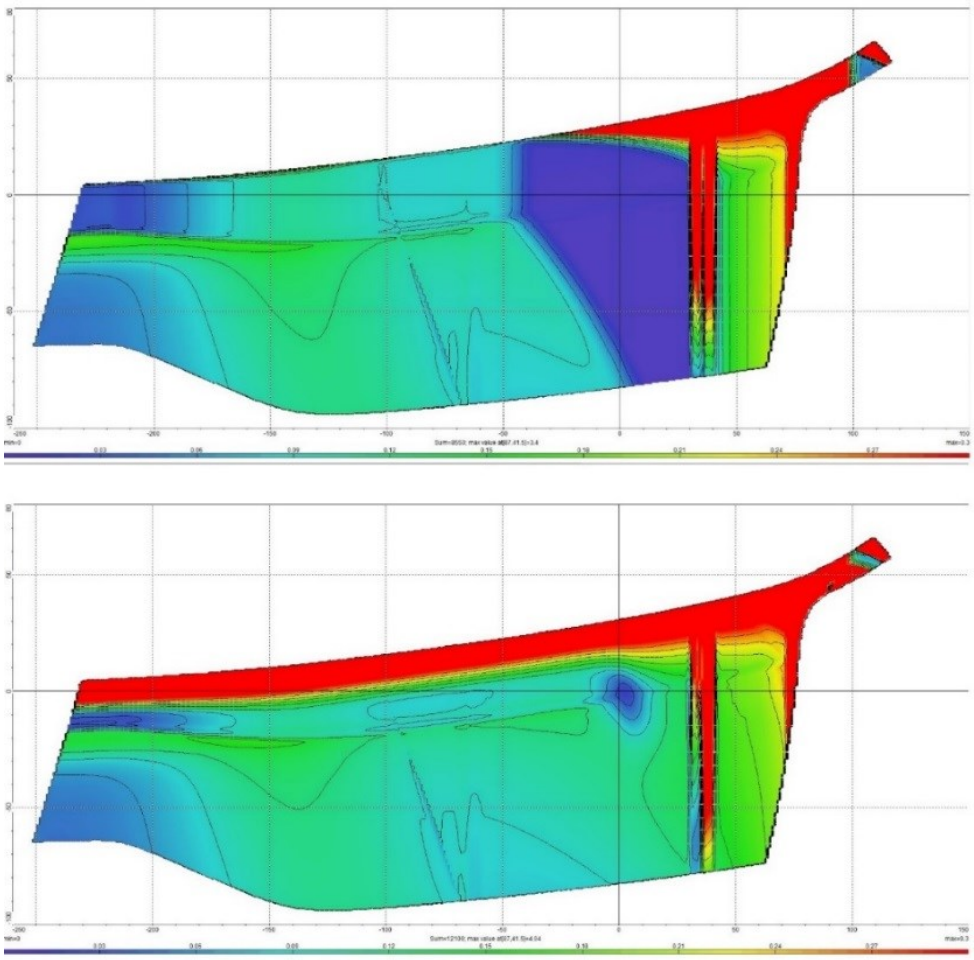

Figure 48: Comparison of total ray deviation between two optimized surfaces

In this ray deviation analysis we can see significant changes, but the defect on the right side is still there, as we can see in Figure 49, so we must use something else to get rid of this defect.

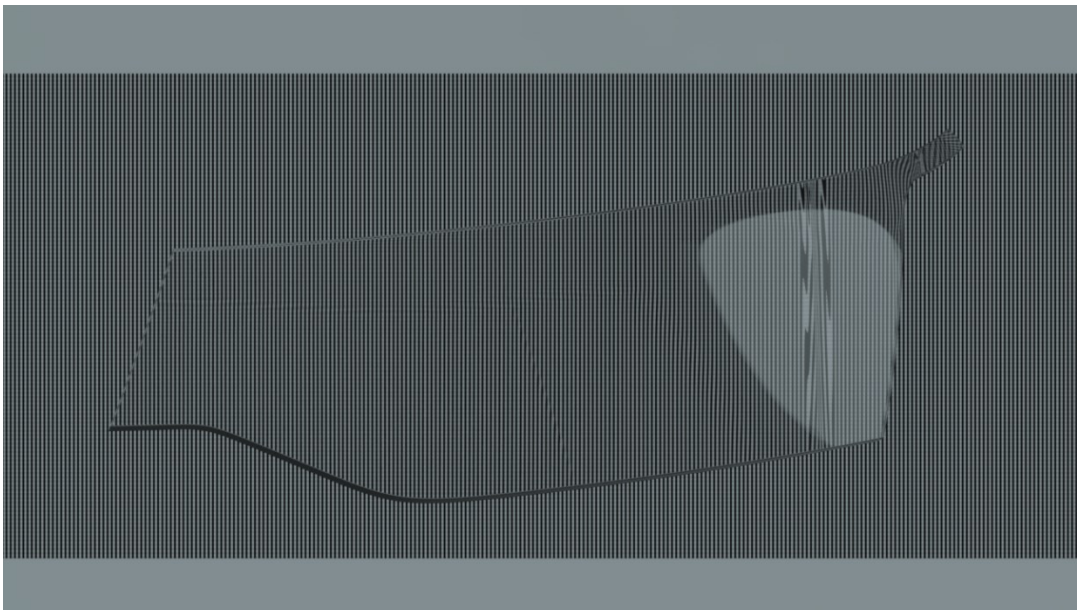

Figure 49: Viewing properties of optimized glass

6.3.1. Different method for optimization

Using different methods and approaches we have probably discovered the correct way to obtain desired results. Its secret lies in CATIA software and the function is called Surface Simplification. This function is not included in regular CATIA package, it needs to be obtained by special license called Generative Shape Optimizer as it is shown in Figure 50.

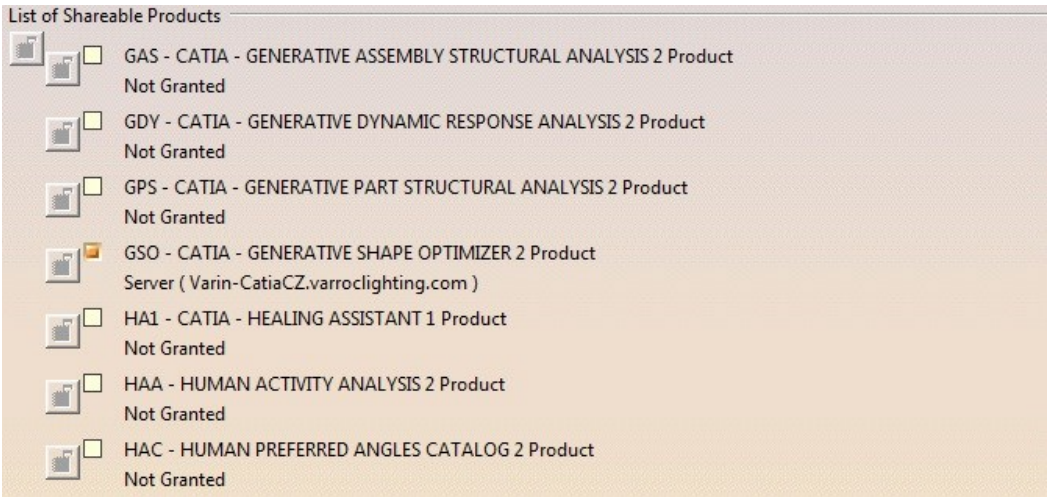

Figure 50: Generative Shape Optimizer license

We use this function to create one single surface for our outer surface, which will be modified later. If there is glass made of too many different parts, not everytime is this function applicable. This can be solved by saving the glass in .igs format, then open it again in CATIA and after that it should work. Another solution is to use Join function with lower Merging distance.

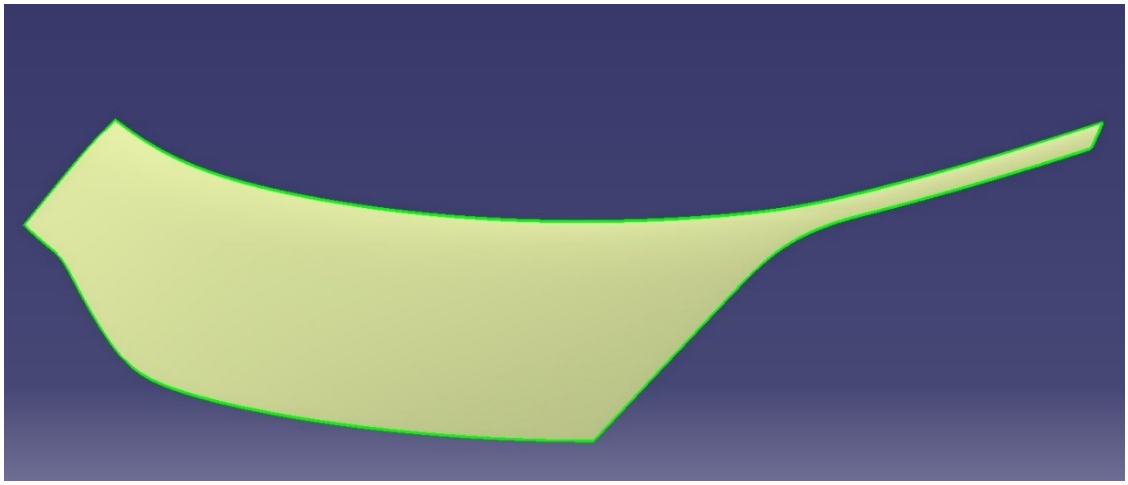

Figure 51: One single surface made from Surface Simplification

Now we apply the function Untrim on our surface and then with function Extrapolate we expand it to required size, which should be ready for optimization in EXPOSE software.

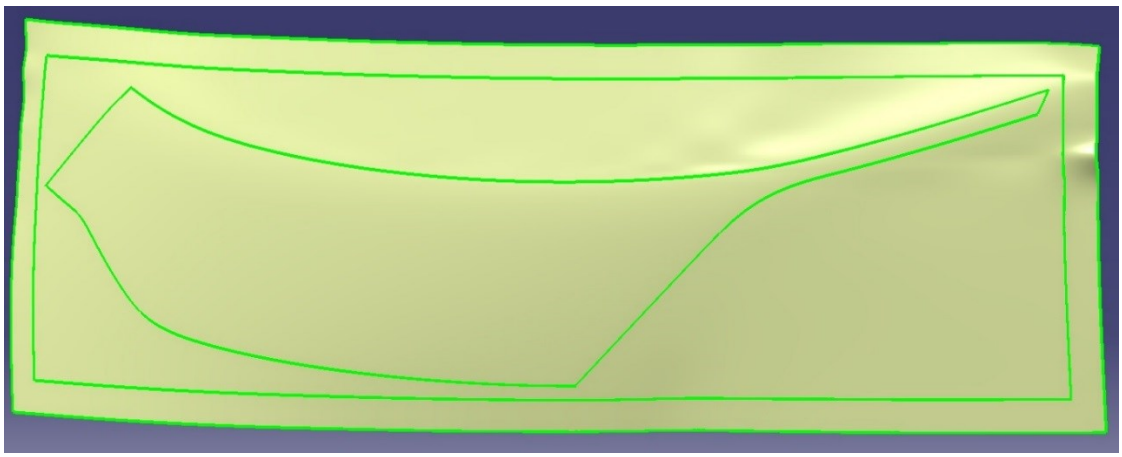

Figure 52: The final surface for EXPOSE software

From this outer surface we make inner surface with function Offset and then start optimization in EXPOSE software with the same settings as in the first case. The result of ray deviation is shown in Figure 53.

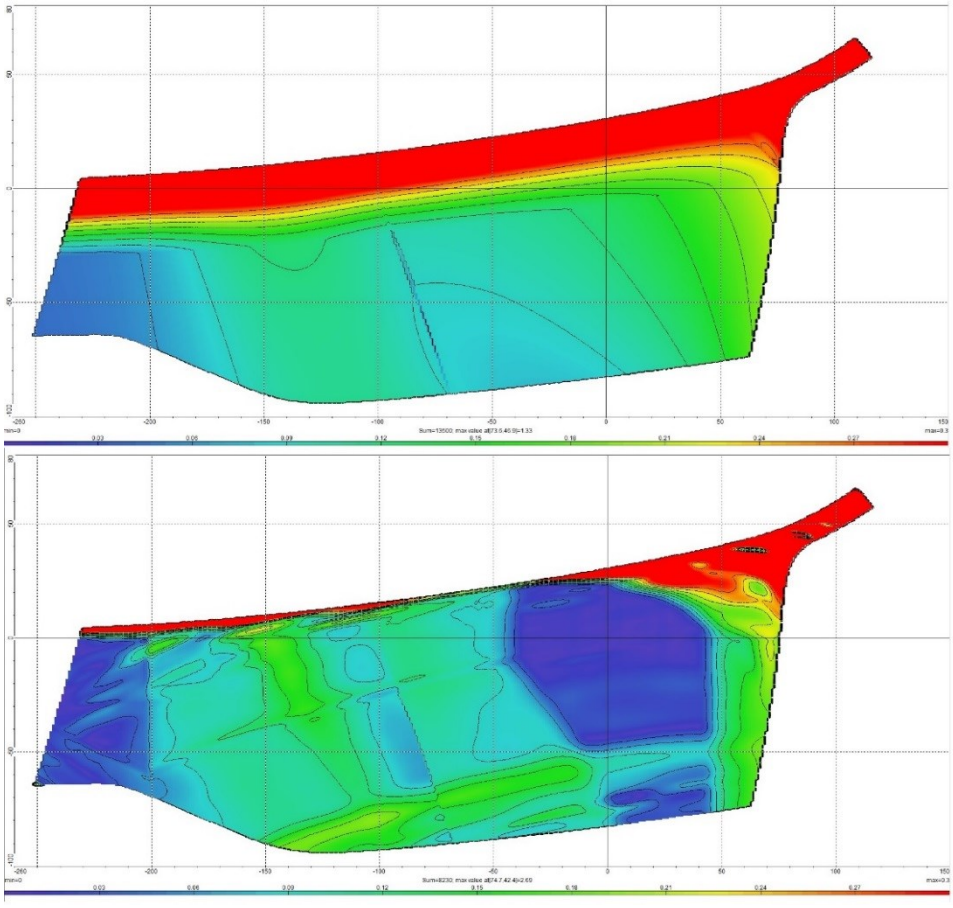

Figure 53: Comparison of total ray deviation

We can see significant improvement, but what matters the most at this time is the result of viewing properties which is displayed in Figure 54.

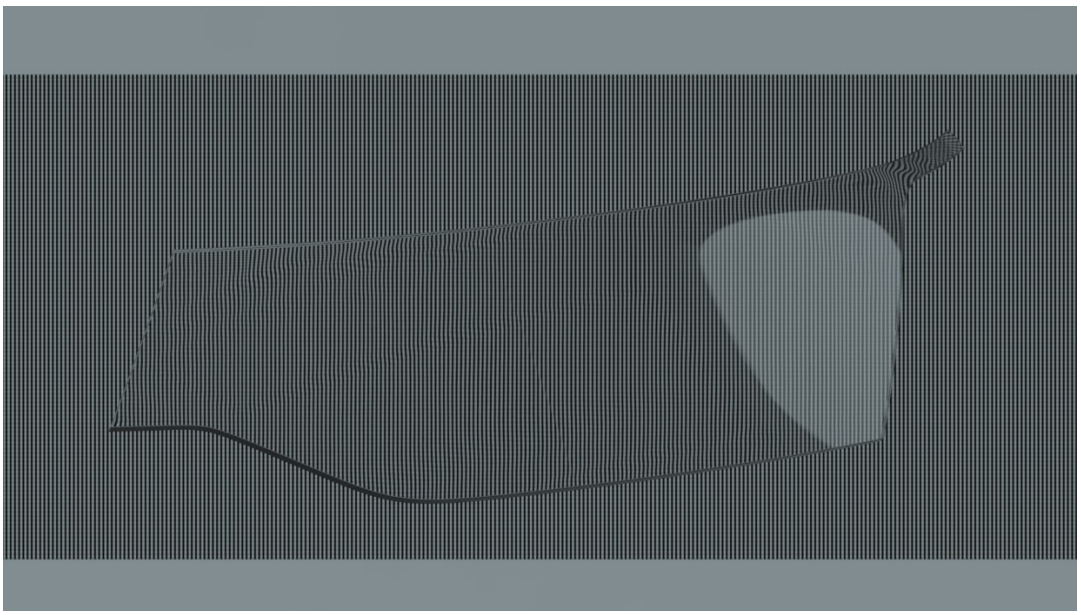

Figure 54: Viewing properties of optimized glass

Finally we have obtained optimized glass with no visible defect which can be used. We can also check the wall thickness analysis to see where are the differences in thickness in our optimized glass and the map of light intensity, both of these analyses are shown in Figures 55 and 56, separately.

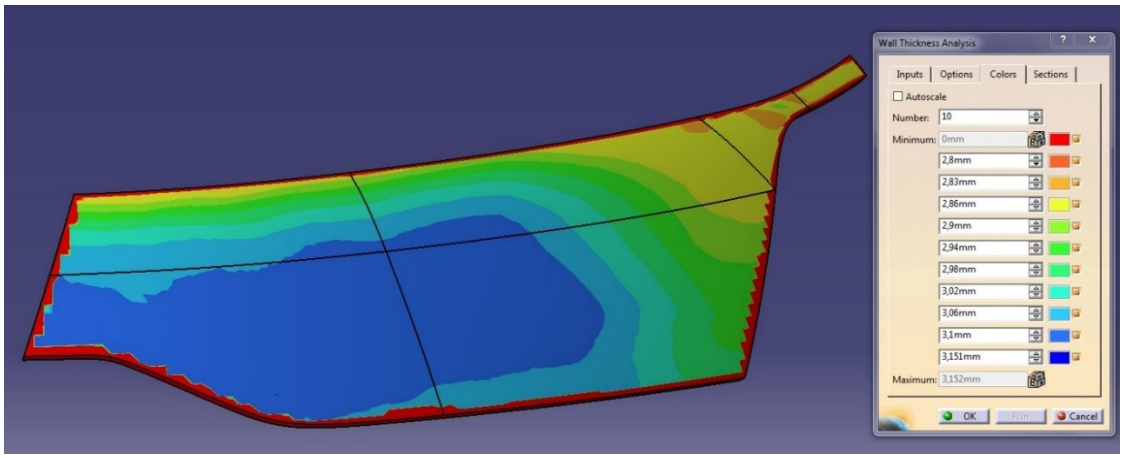

Figure 55: Wall thickness analysis

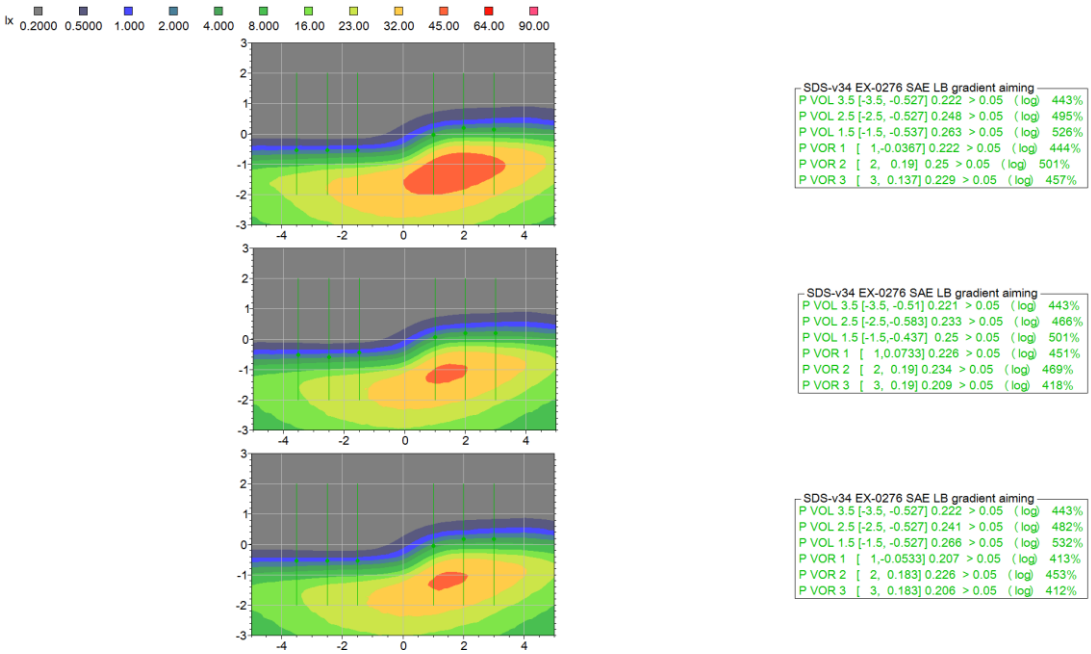

Figure 56: Analysis of map of light intensity

6.4. Results of optimization

Another examples of our functioning method are shown below in Figures 57-61, we can safely say that our method is working properly and that we can create optimized glass with improved properties regarding deviation of rays and position of maximum light intensity.

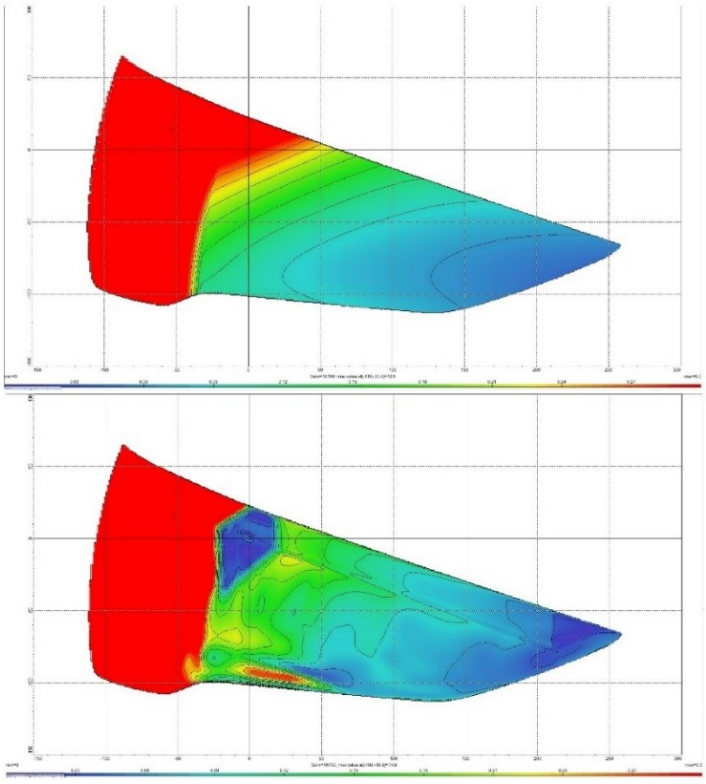

Figure 57: Comparison of total ray deviation

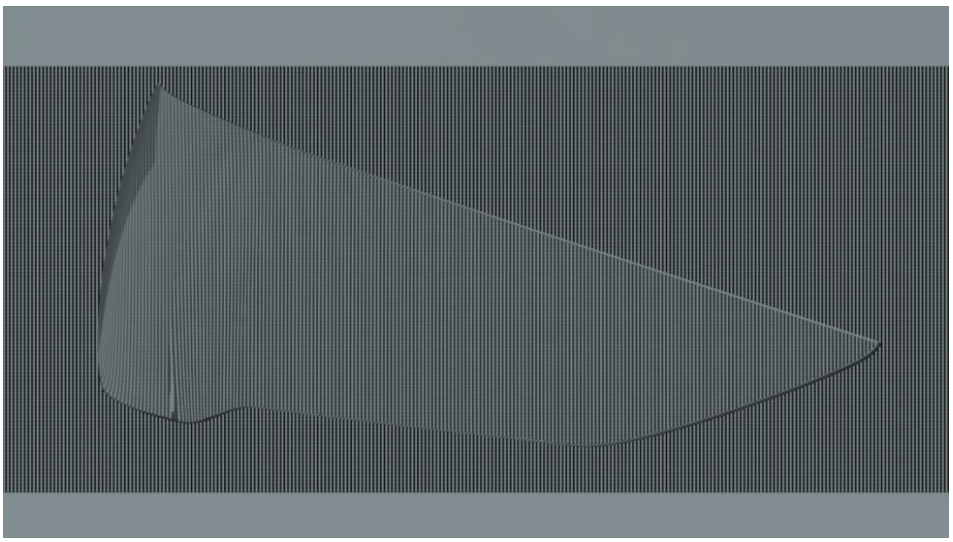

Figure 58: Viewing properties of glass made from parallel surfaces

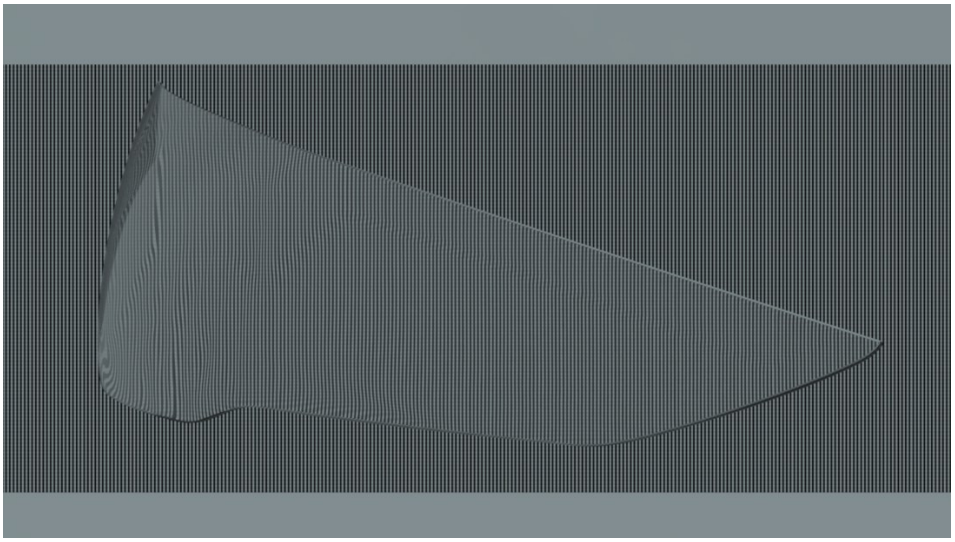

Figure 59: Viewing properties of optimized glass

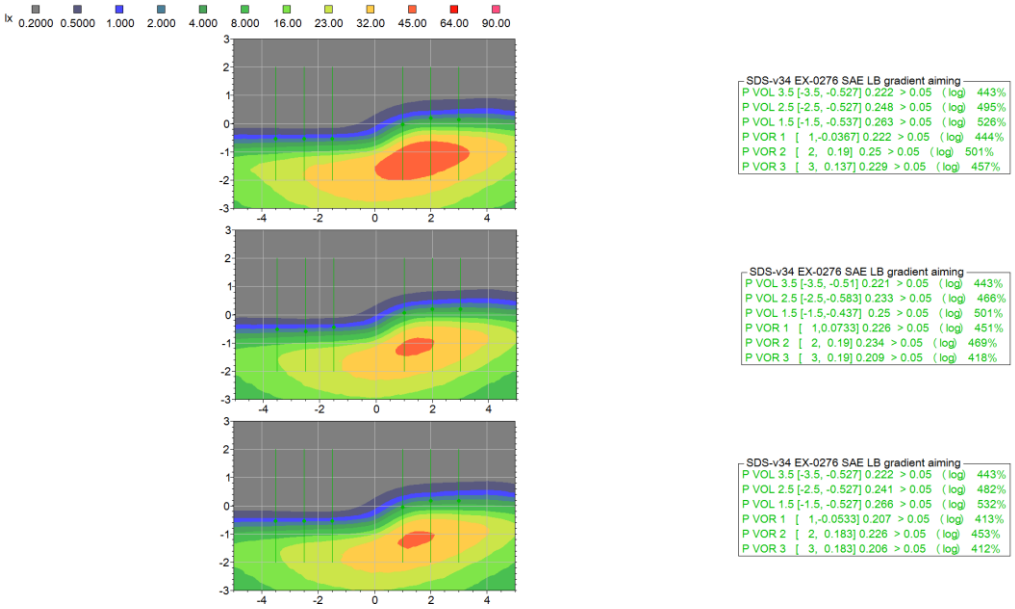

Figure 60: Analysis of map of light intensity

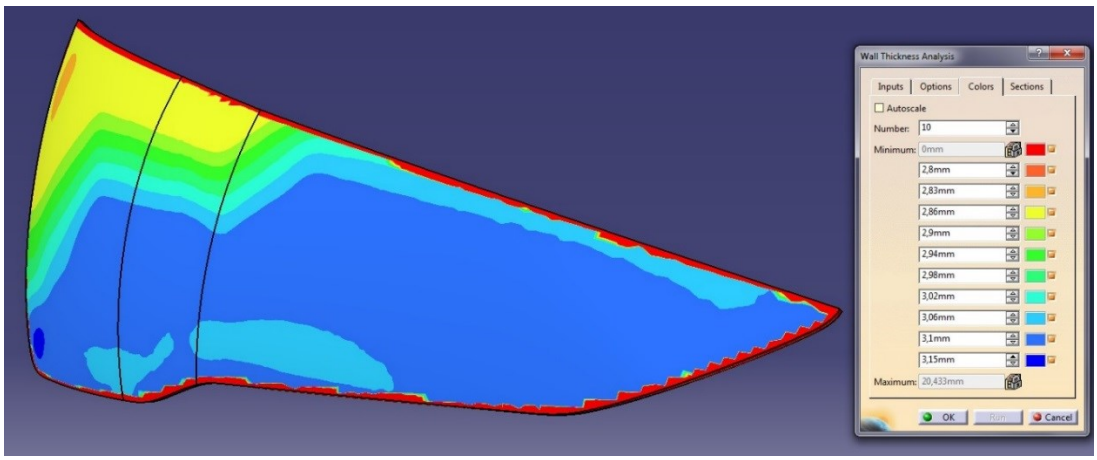

Figure 61: Wall thickness analysis

6.5. Cooperation on upcoming project

During my stay at Varroc Lighting Systems, s.r.o. we have participated on a real upcoming project in a cooperation with an Indian branch. They had issues with optimization of cover glass that had quite a peculiar design, as it is shown in Figures 62 and 63 and so they asked us to help them with optimization.

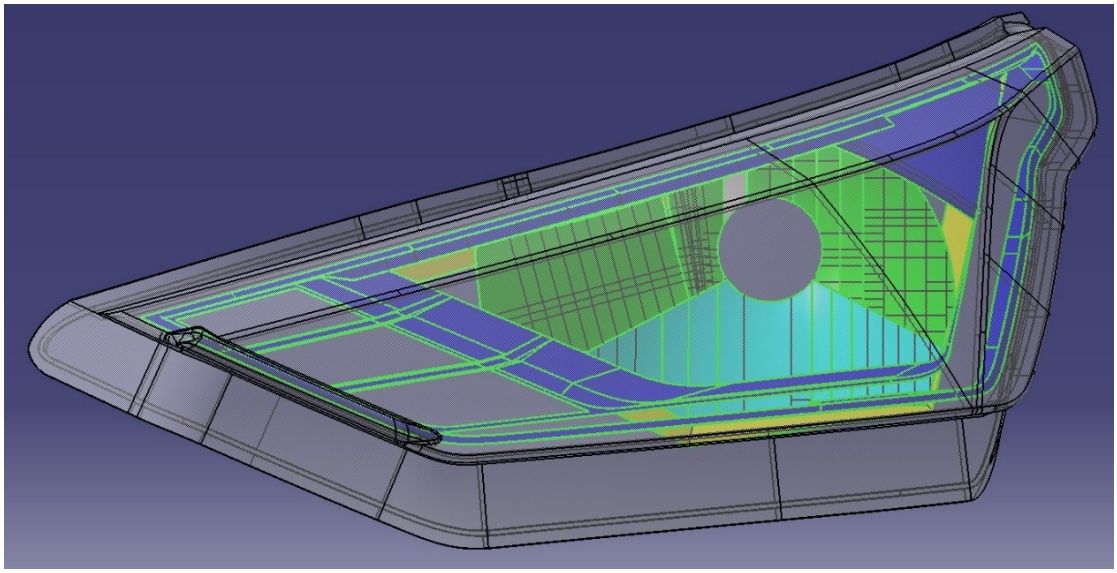

Figure 62: The whole design of the headlamp

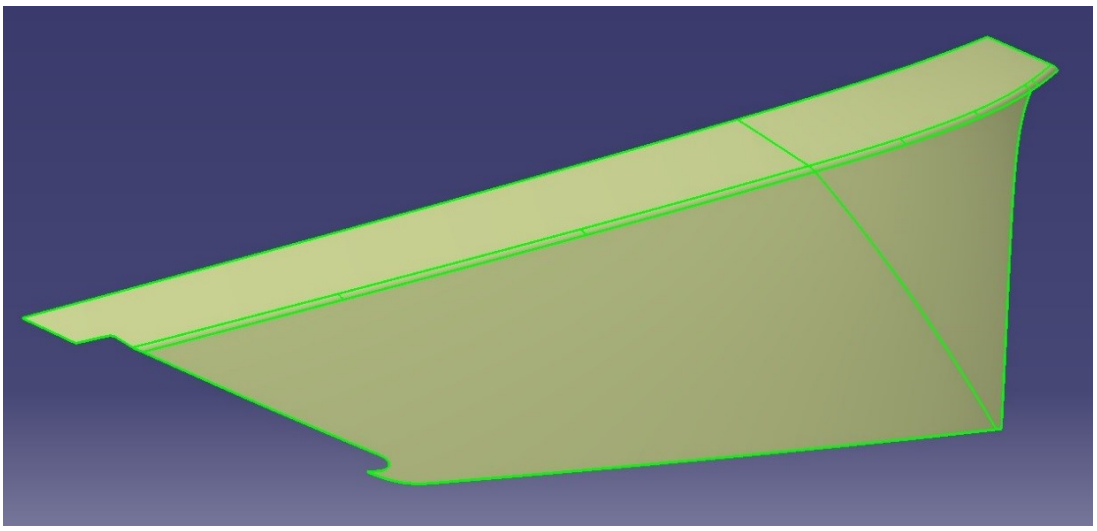

Figure 63: Lens of the headlamp which will be optimized

One of suggestions from Indian team was to change the outer surface and make a whole new design, as it is shown in Figure 64, but their design did not fulfill photometric requirements, so another solution for improvement was needed.

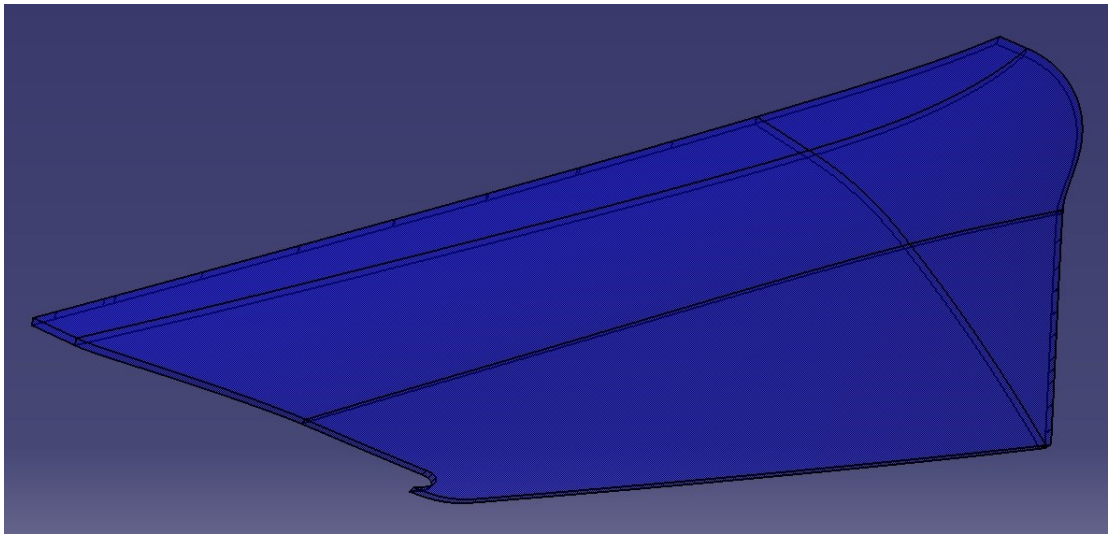

Figure 64: Suggestion for the new shape of lens

At first we started to optimize the suggested new shape, the results were better as it is shown in the comparison of analyses of ray deviations in Figure 65, but we were not satisfied with it, so we started to optimize original surface.

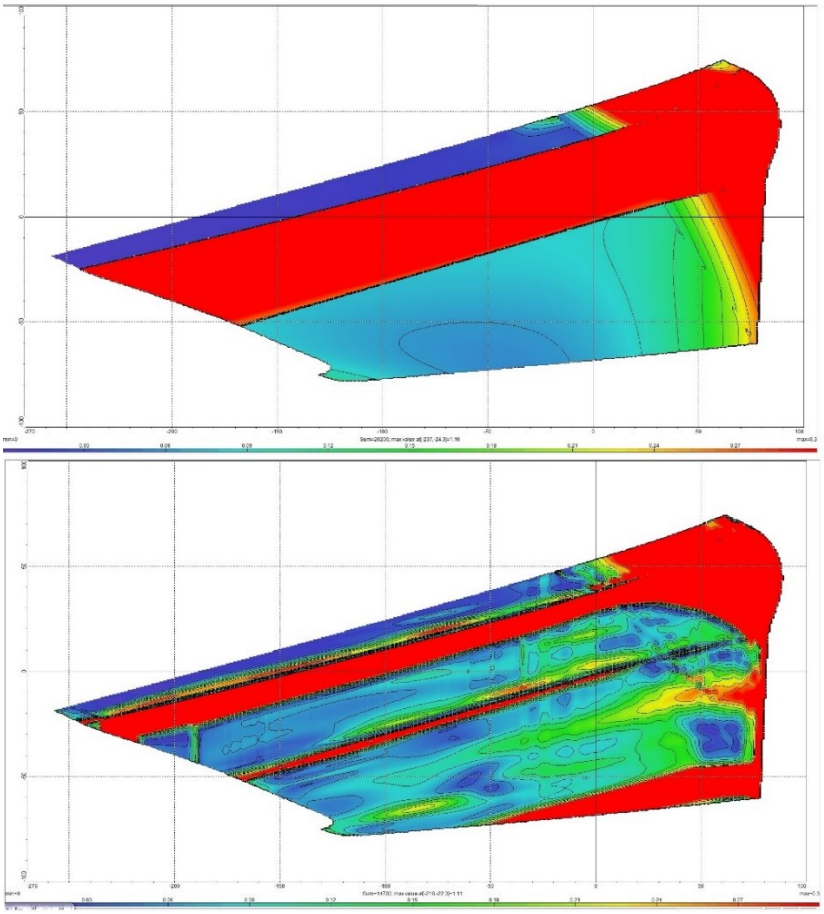

Figure 65: Comparison of ray deviations of first suggestions

The troublesome part of this lens was the small transition part between bigger surfaces. When we optimized the whole surface the results were not bad, but there was still a room for an improvement, so we separated upper and lower part of this lens, optimized each separately and then put to one window in CATIA software, at it is shown in Figure 66.

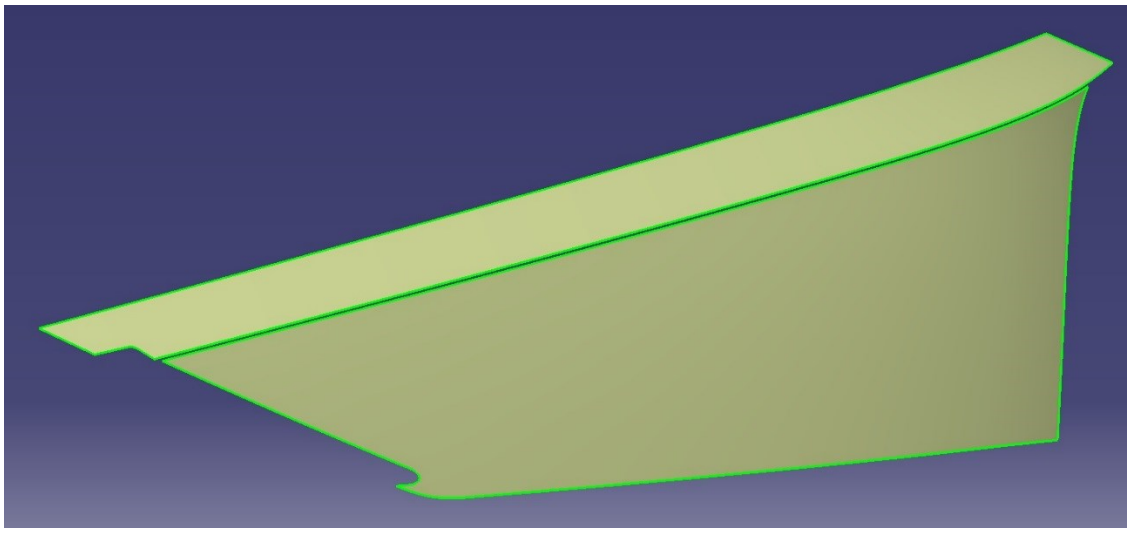

Figure 66: Separated optimized surfaces

We can see the hole in a place where the troublesome part was. Now it was task for us to connect upper and lower part of this lens. We extrapolated each surface and then with function Trim made a single surface. From the original surface we discovered that the troublesome part has radius of 5,26 mm so with the function Edge Fillet we created the transition surface with the same radius. Our new suggested inner surface is shown in Figure 67.

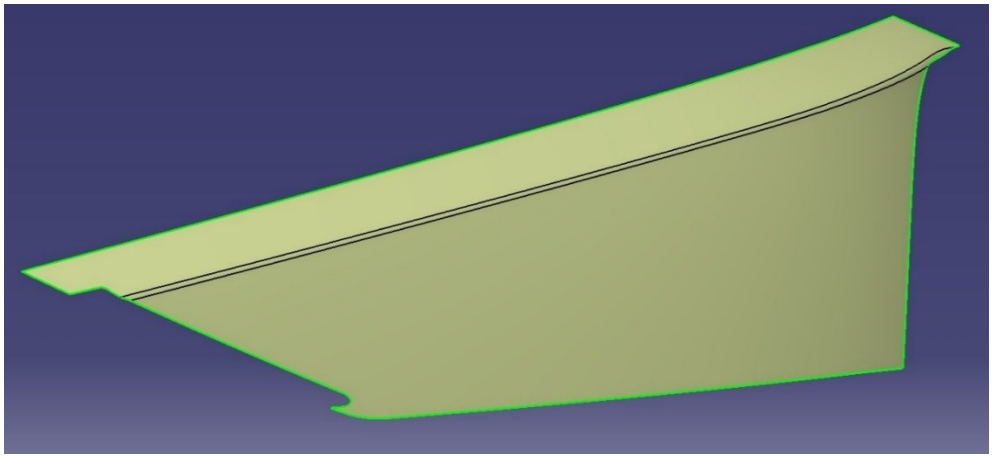

Figure 67: New suggested inner surface

At this point that we created new optimized lens it is time for analysis. At first let us look at analysis of ray deviations, which is displayed in Figure 68.

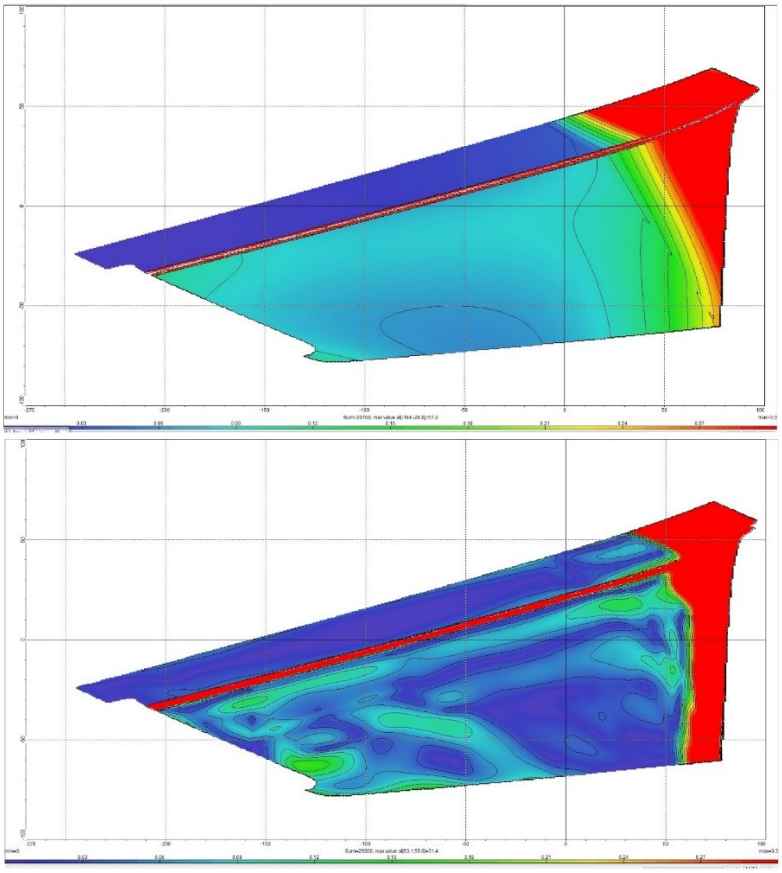

Figure 68: Comparison of ray deviations

We can see that our optimized glass exhibits much better results regarding ray deviation. Very important suspect is viewing properties of these cover glasses, Figures 69 and 70 show comparison between unoptimized and our optimized glass.

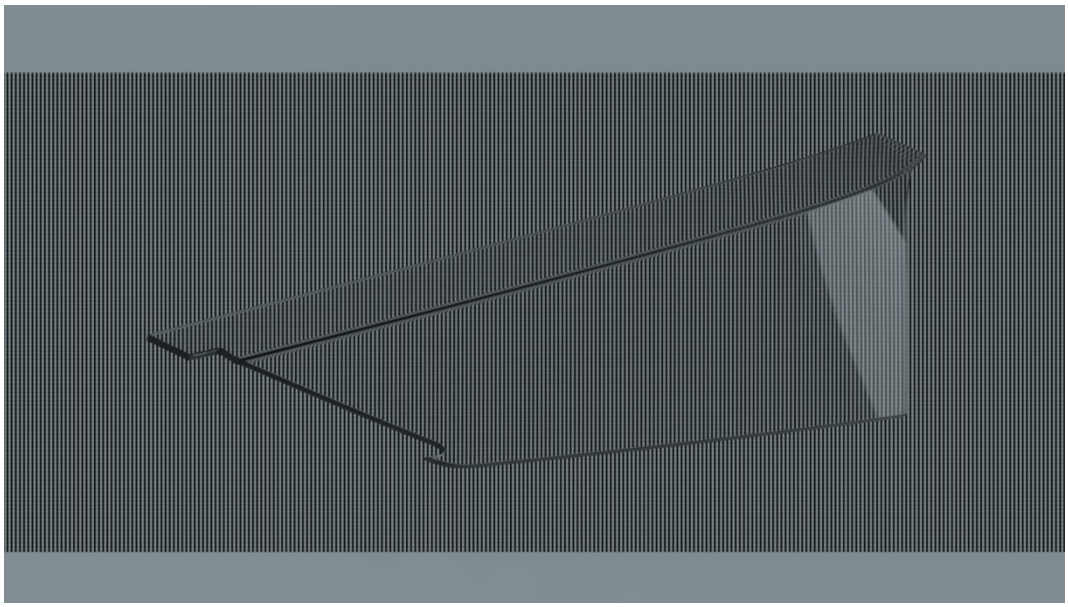

Figure 69: Viewing properties of unoptimized glass

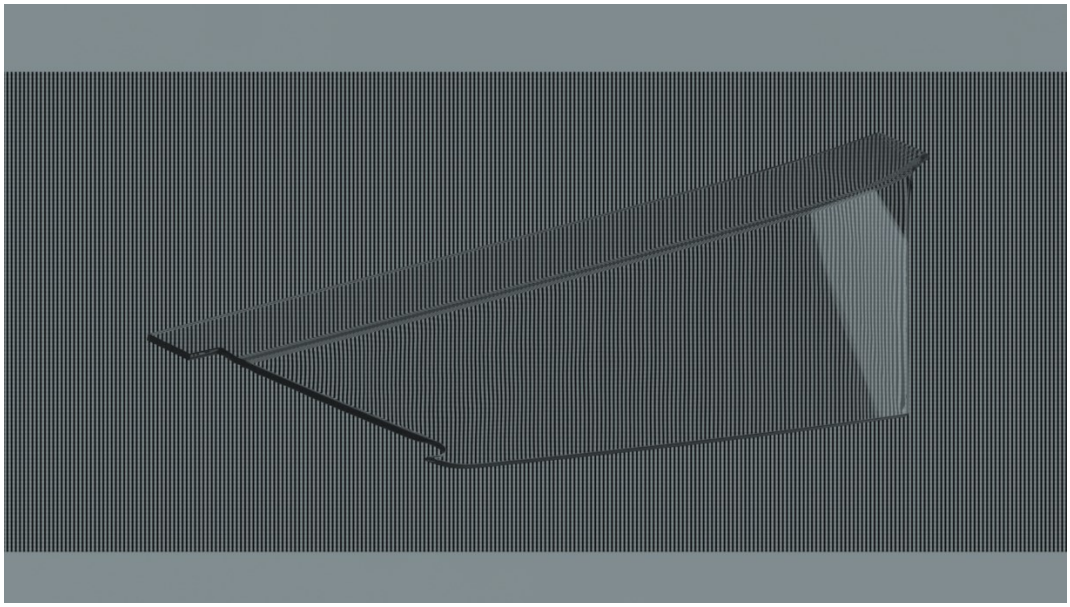

Figure 70: Viewing properties of our optimized glass

There is not any obvious difference, just a little bit in troublesome part of the lens, but the optimized glass looks better and as we saw earlier it has better properties regarding ray deviation, that means we have created optimized glass with better results.

6.6. Optimization of cover glass with different software

We can optimize lens using another software except of EXPOSE and that is LucidShape, the software where the analysis is made, but as it will be shown, it is not that efficient and therefore it is not very useful. In this optimization one cannot choose the minimal and maximal thickness and outer surface of lens must be made of one single part in CATIA software – this can be done using Surface Simplification function in CATIA software. Computing time of optimization in LucidShape software is much shorter than in EXPOSE software which indicates that the results will not be as good as from EXPOSE software. Figure 71 shows ray deviation analysis of optimized surface from LucidShape software.

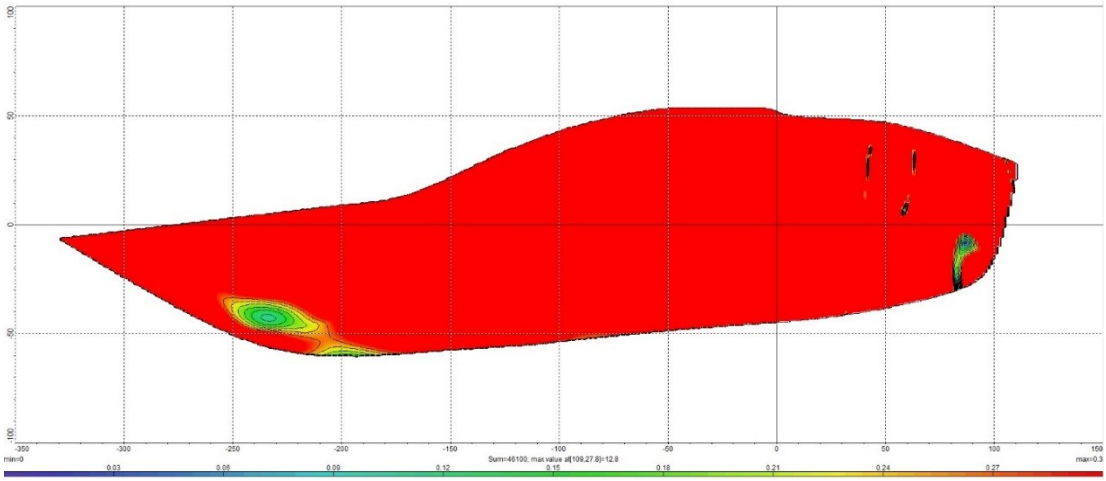

Figure 71: Ray deviation analysis of optimized surface from LucidShape

We can see that this optimization is terrible and cannot be used. Moreover, the thickness analysis shown in Figure 72 displays that maximal thickness used in this optimization is 4,36 mm, which cannot be possible when we consider that start thickness was 3 mm.

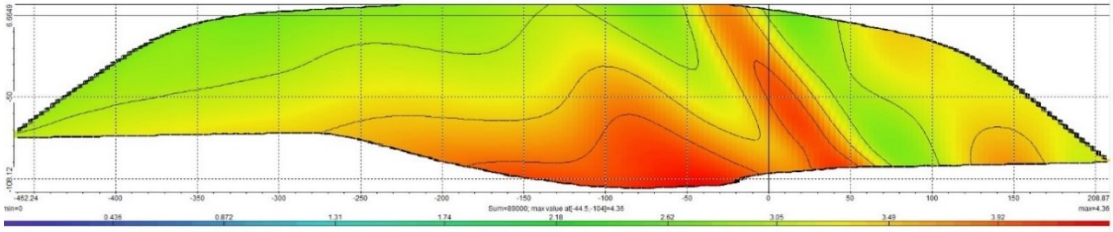

Figure 72: Thickness analysis of optimized surface from LucidShape

7. Conclusion and perspectives

The purpose of this diploma thesis was to perform a description and optimization of front glass in car lighting. Both topics were sufficiently included and the outcome was the creation of guideline for optimization of cover glass and discussion of results and used methods. We believe that we have managed to obtain functioning method for optimization combining theoretical knowledge of headlamps, analytical relations of beam deviation and practical skill with computer-aided design and required software.

With a considerable amount of analyses we proved its functionality, which we have shown on several examples. The original results of master thesis are derivation of general formula for beam deviation in cover glass (Equations 5.9 – 5.10), a new method of optimization of cover glass using special functions in CATIA software and the summary of optimization procedure in the comprehensive guideline.

Due to a nondisclosure agreement with the company Varroc Lighting Systems, s.r.o., we could not include all technical aspects of the optimization in the public version of this thesis. Extended version of the guideline is available for those who are interested in company Varroc Lighting Systems, s.r.o.

Regarding the perspectives, our following steps are to remain in cooperation with company Varroc Lighting Systems, s.r.o. to improve our method for optimization of cover glass and start to focus on another areas of interest in car lighting industry, for example improved shapes of reflector systems, materials with enhanced reflectance or new light sources.

8. References

[1] MOORE, D. W. *Headlamp History and Harmonization.* Ann Arbor: University of Michigan Transportation Research Institute, 1998. Technical Report No. UMTRI-98-21

[2] STERN, D. J. *Headlamp aiming specifications & procedures*. 2009. Informal document No. GRE-68-20

[3] WÖRDENWEBER, B., J. WALLASCHEK, P. BOYCE and D. HOFFMAN. *Automotive Lighting and Human Vision*. Springer-Verlag Berlin Heidelberg, 2007. ISBN 978-3-540-36696-6. DOI 10.1007/978-3-540-36697-3

[4] WIKIMEDIA COMMONS. Headlight lens optics schematic. *Commons. wikimedia.org* [online]. San Francisco (CA): Wikimedia Foundation, © 2005. [cit. 2017-11-16] Available from: https://commons.wikimedia.org/w/index.php? curid=249247

[5] DARSTEN TONGUE. Hella Headlamp Systems. *Dastern.torque.net* [online]. © 2014. [cit. 2017-12-07] Available from: http://dastern.torque.net/techdocs/ Archives/Hella_Systems/hella_head lamp_systems.htm

[6] SALEH, B. E. A. and M. C. TEICH. *Fundamentals of photonics*. 2nd ed. Hoboken, N.J.: Wiley Interscience, 2007. ISBN 978-0-471-35832-9

[7] BRADY, D. J. *Optical imaging and spectroscopy*. Washington, D.C.: Optical Society of America, 2009. ISBN 978-0470048238

[8] WIKIMEDIA COMMONS. Philips H7 12V 55W. *Commons.wikimedia.org* [online]. San Francisco (CA): Wikimedia Foundation, © 2007. [cit. 2018-01-02] Available from: https://commons. wikimedia.org/w/index.php?curid=2358798

[9] LENK R. and C. LENK, *Practical lighting design with LEDs*. Second Edition. Piscataway, NJ: John Wiley & Sons, 2017. ISBN 978-1-119-16531-6

[10] ZHELUDEV, Nikolay. The life and times of the LED – a 100-year history. *Nature Photonics*. 2007, roč.1, č.4, s. 189-192. ISSN 1749-4885. DOI: 10.1038/nphoton. 2007.34

[11] WIKIMEDIA COMMONS. PnJunction-LED-E. *Commons.wikimedia.org* [online]. San Francisco (CA): Wikimedia Foundation, © 2011. Available from: https://commons. wikimedia.org/w/index.php?curid=14985902

[12] SKABARDONIS, J. *Automotive head lamp lenses made of Makrolon*. *Ledsmagazine.com* [online]. © 2014 [cit. 2018-02-19] Available from: http://www.ledsmagazine.com/ugc/2014/12/04/awardwinning-f150-led-head lamps-molded-with-bayer-polycarbonate.html

[13] COVESTRO PLASTICS. Makrolon: Product range and typical values. *Plastics.covestro.com* [online]. © 2018 [cit. 2018-05-01]. Available from: https:// www.plastics.covestro.com/en/Library/Product-brochures

[14] NATIONAL PHYSICAL LABORATORY. Principles of Photometry. *Npl.co.uk* [online]. © 2011. [cit. 2018-02-27] Available from: http://www.npl.co.uk/upload/ pdf/Principles%20of%20Photometry.pdf

[15] LIN, I. Showcase: A brief introduction of LED bulbs 2010. *BeLight*. 2010, č.3, s.10-12. ISSN 2074-0751

[16] COLOUR & VISION RESEARCH LABORATORY. Scotopic luminosity curve. *Cvrl.org* [online]. © 2014 [cit. 2018-03-01]. Available from: http://www.cvrl.org/ database/text/lum/scvl.htm

[17] COLOUR & VISION RESEARCH LABORATORY. 2-deg colour matching functions. *Cvrl.org* [online]. © 2014 [cit. 2018-03-13]. Available from: http://www. cvrl.org/database/text/cmfs/ciexyz31.htm

[18] ENCYCLOPAEDIA BRITANNICA. Luminous intensity. *Britannica.com* [online]. © 2005 [cit. 2018-03-22]. Available from: https://www.britannica. com/science/ luminous-intensity

[19] DR. DR. BILL'S PAGE. Illuminance. *Drdrbill.com* [online]. ©1992 [cit. 2018-03-28]. Available from: http://www.drdrbill.com/downloads/optics/photometry/ Illuminance.pdf

[20] LIGHTING DESIGN GLOSSARY. Luminance. 2009. *Schorsch.com* [online]. © 2009 [cit. 2018-04-01]. Available from: http://www.schorsch.com/ kbase/glossary/ luminance.html

[21] STIMSON, A. *Photometry and radiometry for engineers*. New York: Wiley, 1974. ISBN 978-0471825319

[22] DUGGAL, V., A. ZOLI and S. RUSH. *CADD primer: a general guide to computer aided design and drafting: CADD, CAD*. New York: Mailmax Pub., 1999. ISBN 978-0962916595

[23] NARAYAN, K. L, K. M. RAO and M.M.M. SARCAR. *Computer aided design and manufacturing*. New Delhi: Prentice-Hall of India, 2008. ISBN 9788120333420

[24] DASSAULT SYSTÉMES. Discover CATIA. *3ds.com* [online]. 2015 [cit. 2018-04-01]. Available from: https://www.3ds.com/products-services/catia/

[25] ISICAD. The Dassault systemes Success Story. *Isicad.net* [online]. © 2010 [cit. 2018-04-03]. Available from: http://isicad.net/articles.php?article_num=14120

[26] SYNOPSYS. LucidShape: Innovative Automotive Lighting Design. *Synopsys.com* [online]. © 2018 [cit. 2018-04-09]. Available from: https://www.synopsys.com/optical-solutions/lucidshape/lucidshape.html

[27] LUXRENDER. LuxRender simulations. *Luxrender.net* [online]. © 2007 [cit. 2018-04-20]. Available from: http://www.luxrender.net/en_GB/index

[28] SYNOPSYS. LightTools Illumination Design Software. *Synopsys.com* [online]. © 2018 [cit. 2018-04-09]. Available from: https://www.synopsys.com/optical-solutions/ lighttools.html

9. List of figures

10. List of tables